

2/22/96

# SANDIA REPORT

SAND95-2105 • UC-404  
Unlimited Release  
Printed December 1995

RECEIVED  
MAR 04 1996  
OSTI

## Chemical Vapor Deposited Diamond-On-Diamond Powder Composites (LDRD Final Report)

Janda K. Panitz, Wen L. Hsu, David R. Tallant, Mark McMaster, Ciaran Fox, David Staley

Prepared by  
Sandia National Laboratories  
Albuquerque, New Mexico 87185 and Livermore, California 94550  
for the United States Department of Energy  
under Contract DE-AC04-94AL85000

Approved for public release; distribution is unlimited.

Issued by Sandia National Laboratories, operated for the United States Department of Energy by Sandia Corporation.

**NOTICE:** This report was prepared as an account of work sponsored by an agency of the United States Government. Neither the United States Government nor any agency thereof, nor any of their employees, nor any of their contractors, subcontractors, or their employees, makes any warranty, express or implied, or assumes any legal liability or responsibility for the accuracy, completeness, or usefulness of any information, apparatus, product, or process disclosed, or represents that its use would not infringe privately owned rights. Reference herein to any specific commercial product, process, or service by trade name, trademark, manufacturer, or otherwise, does not necessarily constitute or imply its endorsement, recommendation, or favoring by the United States Government, any agency thereof or any of their contractors or subcontractors. The views and opinions expressed herein do not necessarily state or reflect those of the United States Government, any agency thereof or any of their contractors.

Printed in the United States of America. This report has been reproduced directly from the best available copy.

Available to DOE and DOE contractors from  
Office of Scientific and Technical Information  
PO Box 62  
Oak Ridge, TN 37831

Prices available from (615) 576-8401, FTS 626-8401

Available to the public from  
National Technical Information Service  
US Department of Commerce  
5285 Port Royal Rd  
Springfield, VA 22161

NTIS price codes  
Printed copy: A04  
Microfiche copy: A01

## **CHEMICAL VAPOR DEPOSITED DIAMOND-ON-DIAMOND POWDER COMPOSITES** (LDRD Final Report)

Janda K. Panitz, Wen L. Hsu, David R. Tallant,  
Mark McMaster, Ciaran Fox, and David Staley  
Sandia National Laboratories  
Albuquerque, New Mexico

### **Abstract**

Densifying non-mined diamond powder precursors with diamond produced by chemical vapor infiltration (CVI) is an attractive approach for forming thick diamond deposits that avoids many potential manufacturability problems associated with predominantly chemical vapor deposition (CVD) processes. We developed techniques for forming diamond powder precursors and densified these precursors in a hot filament-assisted reactor and a microwave plasma-assisted reactor. Densification conditions were varied following a fractional factorial statistical design. A number of conclusions can be drawn as a result of this study. High density diamond powder green bodies that contain a mixture of particle sizes solidify more readily than more porous diamond powder green bodies with narrow distributions of particle sizes. No composite was completely densified although all of the deposits were densified to some degree. The hot filament-assisted reactor deposited more material below the exterior surface, in the interior of the powder deposits; in contrast, the microwave-assisted reactor tended to deposit a CVD diamond skin over the top of the powder precursors which inhibited vapor phase diamond growth in the interior of the powder deposits. There were subtle variations in diamond quality as a function of the CVI process parameters. Diamond and glassy carbon tended to form at the exterior surface of the composites directly exposed to either the hot filament or the microwave plasma. However, in the interior, e.g. the powder/substrate interface, diamond plus diamond-like-carbon formed. All of the diamond composites produced were grey and relatively opaque because they contained flawed diamond, diamond-like-carbon and glassy carbon. A large amount of flawed and non-diamond material could be removed by post-CVI oxygen heat treatments. Heat treatments in oxygen changed the color of the composites to white.

## CONTENTS

INTRODUCTION .....	1
EXPERIMENTAL .....	3
I. Powder Precursor Formation .....	3
A. Powder Stock .....	3
B. Electrophoretic Deposition.....	3
C. Screen Printing a Diamond Ink .....	5
D. Substrate Material.....	6
II. Chemical Vapor Infiltration.....	7
A. The Hot Filament-Assisted Reactor .....	7
B. The Microwave Plasma-Assisted Reactor .....	8
III. Post Deposition Oxygen Heat Treatments .....	9
IV. Sample Analysis .....	10
A. Visual Examination.....	10
B. Raman Spectroscopy.....	10
C. Microscopy.....	10
D. Additional Analysis.....	10
RESULTS AND DISCUSSION .....	12
I. Powder Precursor Formation .....	12
A. Electrophoretic Deposition.....	12
B. Screen Printing Diamond Powder Inks .....	15
II. Chemical Vapor Infiltration.....	16
A. Hot Filament-Assisted reactor Results .....	16
1. General considerations .....	16
2. Preliminary results .....	17
3. Fractional factorial experimentally designed experiments .....	24
B. Microwave Plasma Assisted Reactor.....	30
1. General considerations .....	30
2. Fractional factorial designed experiments .....	31
a. Methane plus hydrogen experiments.....	31
b. Methyl fluoride plus hydrogen experiments .....	38
C. Additional Analysis.....	43
1. Optical transmittance.....	43
2. Electron emissivity.....	44
3. Electron beam excited fluorescence .....	50
4. Density .....	50
SUMMARY AND CONCLUSIONS.....	51
REFERENCES .....	52

## Figures

1. Raman spectra of three types of extremely fine (~ 0.01 $\mu$ m) shock synthesized "diamond" powder from Dupont Corp. (Mypolex®) and from a defense laboratory in the former U. S. S. R (N-10 and N-10-G).....	4
2. Electrophoretically deposited 0 to 0.5 $\mu$ m non-mined diamond powder.....	14
3. Densified, screen printed precursors.....	18
4. Raman spectra shifts.....	19
5. TEM and SEM analysis of CVI diamond deposits.....	21
6. SEM micrographs of the interior surface on the same hot filament-assisted reactor sample shown in Figure 7.....	22
7. Scanning electron micrographs showing the exterior surface of a free-standing hot filaments assisted CVI diamond/trimodal mix diamond powder composite.....	23
8. Raman spectra of the exterior surface of composites densified in the hot filament assisted-reactor following a fractional factorial experimental design.....	25
9. Raman spectra of the interior surface of free-standing composites densified in the hot filament-assisted reactor following a fractional factorial experimental design.....	26
10. Raman spectra of the exterior surface of predominantly CVD coatings on molybdenum formed in the hot filament-assisted reactor following a fractional factorial experimental design .....	27
11. SEM micrographs showing a 100 $\mu$ m thick high density (trimodal powder mix) diamond green body treated in the microwave plasma-assisted reactor: 900 °C substrate temperature, 1500 W, 50 T, 0.5 % $\text{CH}_4$ plus hydrogen, 22 hours.....	32
12. SEM micrographs of a 100 $\mu$ m thick, extremely porous diamond powder green body.....	33
13. Raman spectra of the exterior surface of composites densified in the microwave plasma-assisted reactor following a fractional factorial experimental design with $\text{CH}_4$ plus hydrogen as the working gas.....	34
14. Raman spectra of the interior surface of free-standing composites densified in the microwave plasma-assisted reactor following a fractional factorial experimental design with $\text{CH}_4$ plus hydrogen as the working gas.....	35
15. Raman spectra of predominantly CVD coatings on molybdenum substrates formed in the microwave plasma-assisted reactor following a fractional factorial experimental design with $\text{CH}_4$ plus hydrogen as the working gas.....	36
16. Raman spectra of the exterior surface of composites densified in the microwave plasma-assisted reactor following a fractional factorial experimental design with $\text{CH}_3\text{F}$ plus hydrogen as the working gas.....	39

## Figures (continued)

17. Raman spectra of the interior surface of free-standing composites densified in the microwave plasma-assisted reactor following a fractional factorial experimental design with CH <sub>3</sub> F plus hydrogen as the working gas.....	40
18. Raman spectra of predominantly CVD coatings on molybdenum substrates formed in the microwave plasma-assisted reactor following a fractional factorial experimental design with CH <sub>3</sub> F plus hydrogen as the working gas.....	41
19. Reflectance from 100 mm thick diamond composites on polished, mirror-like silicon substrates from the hot filament-assisted reactor.....	45
20. Infrared absorptance of diamond composite coating/silicon substrate “windows”.....	46
21. Raman spectra from the exterior surface (reactor working gas side/oxygen flow side) and the interior surface (substrate side-tube furnace quartz pallet side) of freestanding diamond composites produced by the hot filament-assisted reactor. ....	47
22. Raman spectra from the exterior surface (reactor working gas side/oxygen flow side) and the interior surface (substrate side-tube furnace quartz pallet side) of freestanding diamond composites produced by the microwave plasma-assisted reactor. ....	48
23. SEM micrographs showing a free-standing composite from the hot filament-assisted reactor before and after a 600 °C, 1 hr oxygen tube furnace treatment. ....	49

## Tables

1. Qualitative interpretation of Raman and fluorescence data in terms of stress, composition and defects – samples from the hot filament-assisted reactor.....	29
2. Qualitative interpretation of Raman and fluorescence data in terms of stress, composition and defects – samples from the microwave plasma-assisted reactor with CH <sub>4</sub> plus hydrogen as the working gas.....	37
3. Qualitative interpretation of Raman and fluorescence data in terms of stress, composition and defects – samples from the microwave plasma-assisted reactor with CH <sub>3</sub> F plus hydrogen as the working gas. ....	42

# **CHEMICAL VAPOR DEPOSITED DIAMOND-ON-DIAMOND POWDER COMPOSITES**

## **INTRODUCTION**

Chemical vapor deposited (CVD) diamond is currently the focus of numerous and diverse research, development, manufacturing and marketing activities. The combination of extraordinary properties that diamond crystals display, including (1) the highest thermal conductivity (above 30 °K), (2) optical transparency from the near ultraviolet to the far infrared, (3) superlative hardness and (4) exceptional x-ray transmittance promise many unique applications.<sup>1,2</sup> Some applications, e. g. (1) thermal conductors for cooling dense electronic packages, (2) optical windows, and (3) strong, refractory, inert, low density material for load bearing structures require relatively thick diamond coatings or free-standing pieces.

At the present time, there are a number of problems associated with depositing thick, predominantly CVD diamond with properties approaching those of the best natural diamond. Diamond grown from a low pressure vapor phase may be flawed and twinned.<sup>3</sup> Thick, predominantly CVD diamond may possess high levels of intrinsic stress which detracts from mechanical strength and stability.<sup>4</sup> Simple, cost effective techniques for patterning diamond have not been widely developed, although some groups have explored alternate approaches for limiting diamond nucleation to selected areas of a substrate by selective seeding with diamond grit.<sup>5</sup> The surface roughness of predominantly CVD diamond characteristically increases with coating thickness, following a fractal growth structure. It is desirable to develop simple, cost effective technique for smoothing or tailoring this rough surface topography.<sup>6</sup> Typical growth rates are low, 1 to 10  $\mu\text{m}$  per hour.<sup>7</sup> The density of predominantly CVD diamond cannot be varied over a wide range.

In order to circumvent limitations associated with predominantly CVD material, we developed techniques for forming non-mined diamond powder precursors, then densified these structures with chemical vapor infiltration (CVI) diamond. Chemical vapor infiltration diamond can be defined as diamond grown from a vapor phase on diamond particles within the interior of the powder precursors, some distance away from the hot filament or the microwave plasma. Chemical vapor deposited diamond can be defined as

diamond grown from the vapor phase over the top of diamond powder precursor particles or nucleation seeds, in close proximity to the hot filament or the microwave plasma. The two techniques we used to deposit diamond powder precursors were (1) electrophoretic deposition and (2) screen printing a diamond paste. Representative properties of these deposits after densification with CVI diamond are described. This approach yields useful, novel and unique structures, such as patterned or textured films, that are difficult or impossible to produce by chemical vapor deposition alone.

## EXPERIMENTAL

### I. Powder Precursor Formation

#### A. Powder Stock

General Electric Corp., (GE Diamond Products, Worthington, Ohio) supplies non-mined diamond powder with a wide range of particle sizes from less than 0.5  $\mu\text{m}$  to 80  $\mu\text{m}$ . General Electric forms diamond at high temperatures and high pressures using proprietary techniques first developed in the 1950's. They have perfected their process to the point that non-mined diamond matches or exceeds the quality of the best ("Type IIa") natural diamonds. Unlike G. E.'s non-mined diamond powder, the properties of commercially available natural diamond powder vary substantially depending on where and when it was mined. We used General Electric's non-mined diamond products both for seeding predominantly CVD diamond growth and for forming diamond powder green bodies. (A ceramic "green body" can be defined as a relatively soft, porous mass of ceramic powder which is typically subjected to additional processing that results in densification and hardening).

Recently, extremely fine "diamond" powders with approximately 10 nm diameter average particle sizes have become available in the United States. Dupont Corp. markets ultrafine Mypolex® "diamond" powder. Weapons lab(s) in the former Union of Soviet Socialist Republics developed techniques involving shock waves for producing ultrafine diamond powder. Raman analysis (Figure 1) indicates that this powder is not good quality diamond (contrary to claims made by certain potential distributors). Furthermore, the particles in these powders have such a large electrostatic charge, these materials are almost impossible to handle and incorporate beneficially into any of the processes developed here.

#### B. Electrophoretic Deposition

Useful, electrophoretically active, diamond particle baths can be prepared by mixing 0.5 to 2.5 wt.% non-mined diamond powder with particle sizes below 3  $\mu\text{m}$  in either deionized water, absolute ethanol or reagent grade isopropanol. Uniformity problems occur when water-based baths are used. Ethanol baths produce useful powder deposits, but ethanol is a controlled substance which must be carefully inventoried at national laboratories. For these reasons we elected to work primarily with isopropanol-based baths.

As-received non-mined diamond powder does not readily disperse in water, ethanol or isopropanol. When diamond is added to these liquids, it initially displays erratic

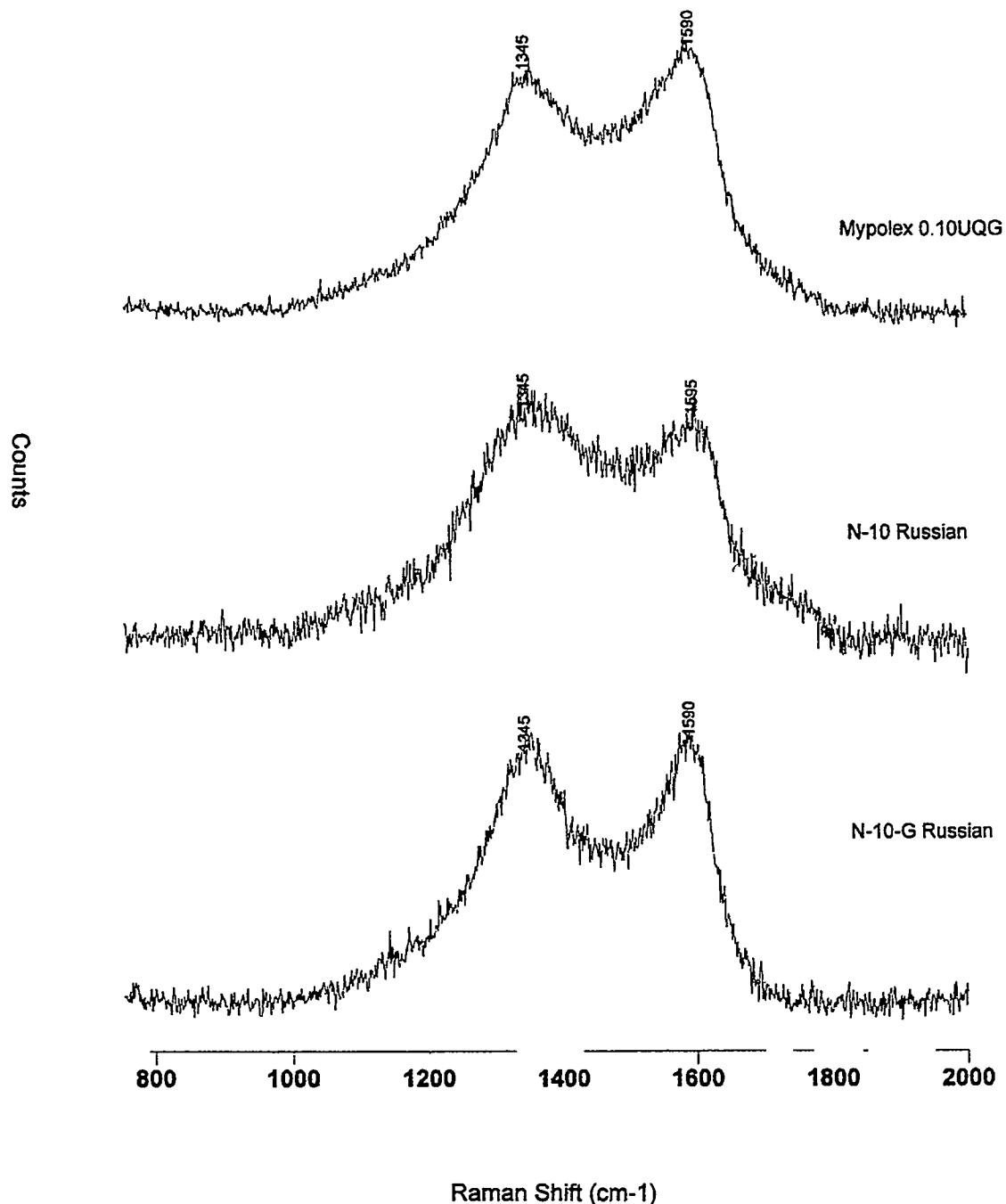


**Figure 1.** Raman spectra of three types of extremely fine ( $\sim 0.01 \mu\text{m}$ ) shock synthesized “diamond” powder from Dupont Corp. (Mypolex®) and from a defense laboratory in the former U. S. S. R (N-10 and N-10-G). All of these samples contain relatively large amounts of glassy carbon ( $\sim 1600 \text{ cm}^{-1}$  Raman shift). X-ray diffraction data (not shown here) indicate Mypolex particles contain diamond cores surrounded by opaque, glassy carbon. N-10 is reportedly prepared by treating N-10-G to remove graphite.

electrophoretic activity. Sonicating these baths for approximately one hour initially then approximately every other day or so during storage (using a 40 KHz ultrasonic cleaner with sufficient power to heat the baths to temperatures from 40 to 70 °C) yields stable electrophoretically active dispersions that stay in suspension, with reproducible properties. These baths can be reused until practically all the diamond powder has been deposited onto substrates if they are periodically sonicated.

Diamond particles below approximately 1  $\mu\text{m}$  in size deposit onto anodically biased substrates. Baths with 2 to 3  $\mu\text{m}$ -sized particles contain both positive and negative charged particles. We generally used baths containing submicrometer-sized particles to deposit diamond onto a variety of positively-biased substrates including silicon wafers and commercial purity nickel sheet.

We typically operated using a fixed voltage of 1000 V across an electrode spacing of 1 to 1.5 cm with electrolyte temperatures of 20 to 40 °C and deposition times of one or two minutes to deposit 50 to 100  $\mu\text{m}$  thick coatings.

### **C. Screen Printing a Diamond Ink**

We prepared diamond inks that were used to screen print patterned diamond powder deposits, 200 to 400 micrometers thick on flat substrates. Our inks contained mixtures of raw stock particle sizes ranging from 54 to 80  $\mu\text{m}$  down to less than half-micrometer. Inks containing a single cut of particle sizes in excess of 2 to 3 micrometers or a multimodal distribution of particle sizes work well for screen printing operations. Particles less than 2 to 3 micrometers in size must be mixed with larger particles to make inks that flow properly during screen printing. We frequently prepared inks with a tri-modal distribution of particle sizes that, in principle, yielded precursors with minimal porosity, i. e. 1 part by weight of a maximum particle size, plus 0.4 parts by weight of a powder with particle sizes approximately equal to 1/10 of the maximum particle size, plus 0.16 parts by weight of a powder with particle sizes approximately equal to 1/100 of the maximum particle size.<sup>8</sup> Inks with a single distribution or a bimodal distribution of particle sizes that yield more porous precursors were used to investigate precursor porosity effects.

We mixed diamond powder with a variety of organic liquids and gels including

1. reagent grade benzyl alcohol,

2. a gel containing approximately 30 wt. % N-22 ethyl cellulose (from Hercules Inc./Aqualon, Wilmington, DE) in reagent grade alpha-terpineol thinned with benzyl alcohol, and
3. a proprietary thick-film vehicle, (“HTSC” from Zyp Coatings, Inc. Oak Ridge, TN).

Approximately 1 part (by weight) powder was mixed with 1 part vehicle plus thinner to form a paste. The composition of this paste was adjusted empirically by adding small amounts of powder or liquid to obtain thixotropic flow characteristics appropriate for screen printing. This paste was then “squeegeed” though patterned openings on 150  $\mu\text{m}$  (0.006 inch) or 300  $\mu\text{m}$  (0.012 inch) thick masks onto silicon or nickel substrates. The wet deposits were air dried at 70 to 90  $^{\circ}\text{C}$ . When vehicles with binders were used, the binder in these preparations was driven off by heating the powder precursors to 450 or 500  $^{\circ}\text{C}$  at  $10^{-6}$  Torr for 15 to 30 minutes in the CVD/CVI reactor immediately before commencing CVI densification.

A number of extremely thick deposits were formed by iteratively printing a 200  $\mu\text{m}$  thick bimodal powder deposit (after shrinkage from a 300  $\mu\text{m}$  mask), densifying, then repeating the printing and densification process.

#### **D. Substrate Material**

Initially, commercial purity nickel sheet and doped silicon wafers were used as substrates. Nickel was used when we wanted to remove diamond composites from the substrate after densification. It is generally known that graphite forms catalytically on a nickel surface. This thin layer of graphite acts as a release layer for the diamond composite. We used silicon substrates when we did not wish to acquire pieces of free-standing diamond. Diamond adheres strongly to silicon substrates because silicon carbide forms at the interior interface. Neither nickel or silicon are appropriate substrates for CVD/CVI diamond chemistries utilizing fluorine or fluorine compounds in the working gas mixture. Fluorine attacks nickel and silicon. Molybdenum was employed as a substrate material midway through this study when we started adding methyl fluoride to the working gas. Fluorine does not aggressively attack molybdenum. After CVD or CVI, pieces of diamond can be removed relatively easily from molybdenum because

1. there is a sufficiently large thermal expansion coefficient mismatch and
2. an integral carbon compound layer does not form.

One project priority was to densify thick diamond deposits. For this reason we performed most of our work with thick ( $> 100 \mu\text{m}$ ) powder deposits formed by screen printing. We printed a number of approximately  $100 \mu\text{m}$  or  $200 \mu\text{m}$  patches of powder on each substrate. We also abraded areas of the substrate with 2 to 4  $\mu\text{m}$  diamond grit, then wiped the area "clean" with an isopropanol soaked swab to seed predominantly CVD diamond growth for comparison with the CVI composites.

## **II. Chemical Vapor Infiltration**

### **A. The Hot Filament-Assisted Reactor**

Diamond powder green bodies were densified in a hot filament-assisted CVD/CVI reactor. The reactor was equipped with a serpentine rhenium filament, spaced 1.5 cm above the 5 cm diameter substrates at closest approach. The filament was operated at temperatures from 2100 to 2300  $^{\circ}\text{C}$ , confirmed with a two-color optical pyrometer. A 5 cm diameter, resistively heated platform with a thermocouple heated substrates to temperatures from 600 to 1100  $^{\circ}\text{C}$ . The reactor vacuum chamber had double stainless steel walls. Water flowed between the inner and outer walls to cool the chamber walls and vacuum seals. Preliminary experiments with a single walled metal reactor indicated the need for water cooling the vacuum chamber. Otherwise the thermal energy required to synthesize diamond heats the walls of a metal reactor to temperatures that burn skin and destroy polymer o-ring seals over extended processing times.

The diffusion-pumped reactor had a background pressure in the  $10^{-6}$  Torr range. After the system had been pumped down to a high vacuum, the substrates were heated to approximately 500  $^{\circ}\text{C}$  for approximately 15 to 30 min. to drive off high vapor pressure residuals, e. g. screen printing ink binders in the powder precursors. System pressure was monitored to assure entrained by-products in the precursors had outgassed. The substrates were then heated to the desired deposition temperature, from 500 to 1100  $^{\circ}\text{C}$  for initial screening experiments, 700 or 825  $^{\circ}\text{C}$  for subsequent fractional factorial designed experiments. The desired ratio of methane and hydrogen was leaked in through two mass flow controllers. The effects of using reactive gas mixtures containing from 0.5 to 2 % ultra high purity  $\text{CH}_4$  plus ultra high purity hydrogen were explored in initial experiments. Subsequent fractional factorial experiments focused on the effects of using 0.5 to 1 % methane plus hydrogen. The high vacuum gate valve was closed, working gas pressure was allowed to leak up to the 50 mTorr range, then the valve to a mechanical pump was opened. The pumping line to the mechanical pump was throttled with a needle valve to stabilize the working gas pressure at 10 or 20 Torr (measured using a baratron gauge).

Then the filament was heated up to 2200 to 2300 °C to thermally decompose the working gas molecules into reactive species and commence diamond deposition.

Environment, safety and health considerations at SNL, NM placed major limitations on the way we operated the hot filament-assisted reactor. Other groups report that good quality hot filament assisted CVD diamond can be deposited at 100 to 200 Torr with deposition rate increasing with gas pressure. Environment, safety and health considerations restrained us from operating our hot filament-assisted reactor at pressures above 20 Torr, however, based on the worst case premise that if the vacuum system failed and the system filled with air, we would be just below the minimum hydrogen concentration resulting in an explosive mixture. Process times extended from 4 to 24 hours for initial exploratory experiments. We later focused on process times of 8 or 16 hours for fractional factorial experiments. Environment, safety and health regulations did not permit us to operate the system unattended. (Some other groups routinely operate reactors unattended, overnight.) Runs exceeding 8 hrs (a 8 hr working day plus 1 hr overtime for pump down and parameter stabilization) were performed over several days of 9 hr shifts.

Early experiments explored a wide range of process parameters that appeared to be of interest based on the results of other groups. A final set of fractional factorial experiments explored the following conditions (and ranges)

1. pressure (10 to 20 Torr),
2. methane concentration (0.5 to 1% in hydrogen),
3. deposition time (8 or 16 hr.), and
4. substrate temperature (700 or 825 °C)

which our initial experiments indicated encompassed optimal conditions for densifying diamond powder green bodies in a hot filament-assisted reactor.

## **B. The Microwave Plasma-Assisted Reactor**

Some powder precursors were densified in a microwave plasma-assisted reactor. The system was equipped with a 2 KW, 2.45 GHz microwave generator, wave guides and tuning system from ASTeX Corp. Microwaves passed through a quartz window into a stainless steel, turbomolecular-pumped vacuum chamber and generated a plasma at working gas pressures. Two inch diameter substrates were clamped against a temperature controlled platform above the plasma “fire-ball”.

This system operated at background pressures in the  $10^{-7}$  Torr range. The substrates were preheated in a hydrogen plasma to drive off high vapor pressure ink by-products before leaking in methane or methyl fluoride to commence deposition. In a microwave plasma-assisted CVD/CVI system, several experimental parameters in combination determine the size and uniformity of the plasma fire ball. Microwave power must be adjusted in combination with gas pressure so the fire ball is uniform over the surface of the substrate and does not touch the walls of the chamber. The microwave plasma fire ball generates a considerable amount of heat; it was typically necessary to reduce the power supplied to the resistive substrate heater during the initial stages of a deposition run to stabilize substrate temperature. Experimental conditions: power, pressure, and substrate temperature, were initially checked and adjusted so system walls, seals, feed-throughs, the quartz microwave inlet window, viewing windows (necessary so the operator can inspect the fire ball and adjust power and pressure), etc. did not reach destructive temperatures. Preliminary experiments indicated that the microwave system could be operated at 0.9 KW at 20 T or 1.5 KW at 50 T, at substrate temperatures of 700 or 825 °C for fractional factorial designed experiments. Two organic gases were used: methane ( $\text{CH}_4$ ) or methyl fluoride ( $\text{CH}_3\text{F}$ ), at concentrations of 0.5 or 1 % in hydrogen. (Working gas mixtures yielding higher fluorine partial pressures rapidly attacked the silicon dioxide viewing window and other parts of the vacuum system.) All fractional factorial microwave plasma-assisted reactor runs were eight hours long. Because the powder precursors were deposited on substrates with a relatively high thermal expansion coefficient and because the substrates were mounted upside-down, the diamond samples tended to fall off their substrate during or after a run. They fell off during runs when their weight increased and exceeded adhesive forces holding them on the substrate. The probability of this happening was reduced by abrading the molybdenum aggressively with diamond grit to roughen the surface to increase hook-and-claw adhesion. The samples were watched during processing. If they fell off prematurely, the run was terminated and repeated. Sometimes the diamond composites fell off after a run was completed while the molybdenum substrate cooled and shrank. The probability of this happening was reduced by turning off the substrate heater very slowly after the conclusion of a run.

### **III. Post Deposition Oxygen Heat Treatments**

After densification in a CVD/CVI reactor, a small number of free-standing samples were heat-treated at 500, 600 or 700 °C in an oxygen tube furnace with ultra high purity oxygen for one or more hours with the hope of “burning-off” non-diamond carbon.

## **IV. Sample Analysis**

### **A. Visual Examination**

After identification, the samples were examined visually and with a low magnification optical microscope to confirm the surface displayed a drussy appearance characteristic micro faceted diamond growth. Adhesion and hardness were qualitatively probed with a sharp stylus. The presence of loose non-cohering, non-adhering diamond powder was interpreted as an indication of incomplete densification.

### **B. Raman Spectroscopy**

Raman spectroscopy is used to measure atomic or molecular polarizability fluctuations characteristic of a material (as opposed to dipole moment fluctuations which give rise to infrared spectra). Many lattice vibrations that occur in different carbon structures give rise to well defined Raman shifts. Raman spectroscopy is an ideal way to analyze the quality of CVD/CVI diamond deposits. The Raman spectra of a large number of representative samples were evaluated to confirm the presence of a narrow band peaking at a Raman shift of approximately  $1331\text{ cm}^{-1}$  which is characteristic of diamond ( $\text{sp}^3$ -bonded tetrahedral carbon). Diamond-like-carbon which is a mixture of  $\text{sp}^2$  and  $\text{sp}^3$  bonded carbon exhibits a broad Raman band near  $1500\text{ cm}^{-1}$ . Glassy carbon, which is also known as nano-crystalline graphite has Raman bands near  $1350\text{ cm}^{-1}$  and  $1600\text{ cm}^{-1}$ . The bandwidth and the frequency perturbation of the Raman shift produced by CVD/CVI diamond coating compared to the sharp  $1331\text{ cm}^{-1}$  shift characteristic of bulk, well-ordered, single crystal diamond can be interpreted as an indication of the amount of residual stress in the CVD/CVI material. Raman spectra and associated fluorescence spectra also indicate the presence of certain impurities and crystallographic flaws.

### **C. Microscopy**

A large number of sample plan-views, cross-sections and interior interfaces were examined using a scanning electron microscope (SEM), to evaluate the shape, size and continuity of surface crystal facets and the amount of porosity in the bulk and at the lower surface. A small number of sample thin-sections were imaged at high magnification using a transmission electron microscope to observe the microstructure of the CVD/CVI diamond growth enveloping non-mined diamond particles.

### **D. Additional Analysis**

The optical transmittance and electron beam induced fluorescence of selected diamond samples and electron emissivity were also evaluated. Visible and infrared transmittances

were measured for representative samples using two standard spectrometers. Selected samples were scanned for evidence of electron-beam-induced fluorescence in an electron microprobe.

In consideration of reports that certain types of diamond, "doped" CVD diamond or diamond-like-carbon have extremely low work functions and/or negative electron affinity, we attempted to measure field emission currents generated from representative samples. Emissivity measurements were made in a vacuum system equipped with a substrate mount that could be biased to several thousand volts with respect to an appertured ground plane placed approximately 1 mm parallel to the sample. Bias voltage was incrementally increased to a maximum test voltage of 2000 V where arcing and breakdown occurred. A channel plate amplifier able to measure emission currents as low as a few nanoamps was used as a detector.

Representative samples were taken to the Center for Microengineered Ceramics at the University of New Mexico with the anticipation of measuring density quantitatively using porosimeters where the samples are immersed in nitrogen or mercury.

## RESULTS AND DISCUSSION

### I. Powder Precursor Formation

#### A. Electrophoretic Deposition

The water-based electrophoretic baths produced rough, irregular, poor quality coatings (Figure 2A). Coating roughness is, in part, due to the relatively low voltage required to dissociate water into oxygen and hydrogen that results in oxygen bubbling over the anodically biased substrate where the negatively charged diamond powder is deposited. Macroscopic coating topography suggests that flocs form, then deposit onto the substrate, inferring that non-mined diamond powder is hydrophobic.

Relatively smooth, uniform, conformal diamond powder coatings can be electrophoretically deposited from ethanol and isopropanol baths (Figure 2B). Threshold voltages of 20 to 50 V across a 1 to 1.5 cm electrode spacing yield visible deposits after approximately 5 to 30 sec. depending on bath concentration. More concentrated baths draw higher current densities and yield faster deposition rates at a given voltage. Nominal coating thicknesses approaching 50  $\mu\text{m}$  (calculated from weight gain and diamond density) can be electrophoretically deposited in 1 min. from a 2.5 wt. % diamond powder plus isopropanol bath operated at a cell voltage of 1000 V across an electrode spacing of 1.5 cm.

The powder particles in these coatings are held together by hook-and-claw adhesion and Van der Waal's forces. Problems occur when the coatings reach a certain thickness and lack sufficient cohesive strength to support their own weight. Stronger coatings form at relatively high electric field strengths, e. g. 1000 V cell voltage across an electrode spacing of 1.5 cm, in high concentration baths (with 2.5 wt. % diamond). Increasing the distribution of particle sizes in the bath serves to increase coating density and cohesive strength, thereby reducing shrinkage and cracking.

Dispersions with more than 2.5 wt. % diamond have undesirable properties. Hard aggregates form during extended storage that cannot be ultrasonically fractured and redispersed. The primary particles in high concentration baths, especially in conjunction with high electric field strengths, tend to floc in the vicinity of the substrate; the density of these flocs causes them to sink before they contact and adhere to the substrate, resulting in partial or no net coating deposition.

Diamond particles tend to deposit first on high field areas, e. g. exterior corners. These initial deposits tend to screen subsequent deposition in these areas and low field areas become coated. Conformal coatings form after some minimum processing time that varies depending on the shape of the substrate (Figure 2C).

It is difficult or impossible to form uniform diamond powder coatings thicker than approximately 200 to 250  $\mu\text{m}$  (Compare Figure 2 Views B and D). There are several effects that work together to limit the maximum thickness of diamond coatings that can be electrophoretically deposited including

- the minimum threshold field strength required for deposition and floc formation at high field areas in combination with
- an increased probability of dielectric flaws with continued deposition,
- coating weight limitations defined by cohesive strength, and
- shrinkage and cracking that occur when the coatings dry.

In summary, attributes associated with electrophoretic deposition of diamond powder precursors include

1. processing speed, simplicity and cost effectiveness,
2. ability to form conformal coatings readily on shaped substrates and
3. opportunities for controlling coating thickness by controlling cell voltage, bath concentration, and deposition time.

Potential problems and complications may arise based on a number of considerations:

1. Substrates must be electrically conductive.
2. Precursor surface smoothness begins to suffer when coatings thicker than 100  $\mu\text{m}$  are formed.
3. Useful precursors thicker than 200 to 250  $\mu\text{m}$  cannot be formed.
4. Opportunities for varying coating porosity (to expedite CVI or form tailored structures) are limited.
5. The dried powder deposits are soft and fragile, which curtails subsequent options for mechanically smoothing or shaping surface topography.

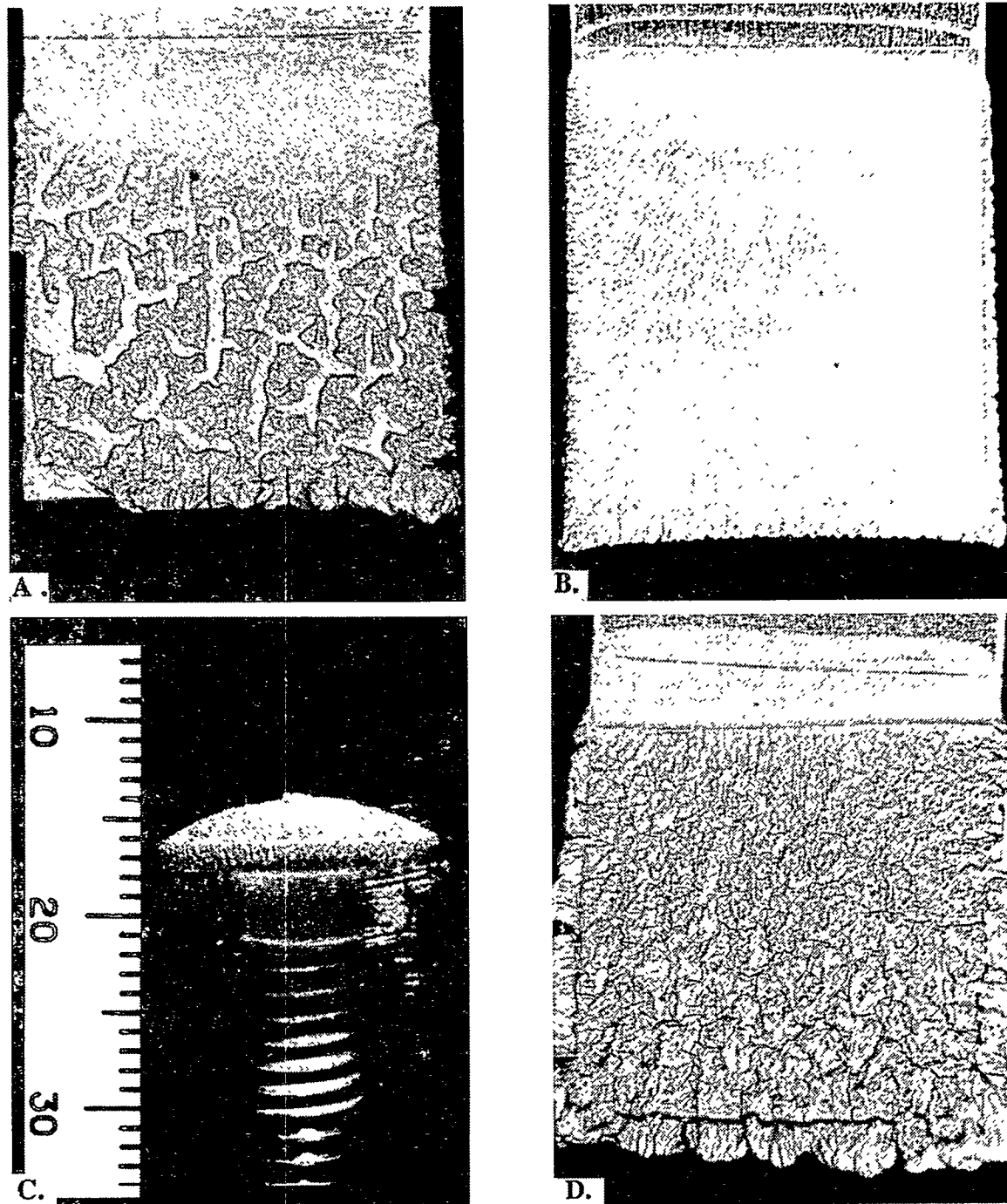


**Figure 2.** Electrophoretically deposited 0 to 0.5  $\mu\text{m}$  non-mined diamond powder. **A.** Reniform clusters from an aqueous bath. **B.** A relatively uniform deposit from an isopropanol bath. **C.** A deposit on a shaped substrate (a steel carriage bolt). **D.** A 250  $\mu\text{m}$  nominal thickness deposit from an isopropanol bath.

## B. Screen Printing Diamond Powder Inks

Many potential problems and limitations associated with electrophoretic deposition (enumerated above) can be avoided by screen printing or painting a diamond powder containing ink or paste. Inks generally contain powder dispersed in a liquid vehicle which may include dissolved material that acts as a binder after the ink dries. The rheological properties of an ink are critically important in any printing or painting operation. Ink flow properties depend on vehicle composition, concentration and particle size. Our immediate objectives were

1. to demonstrate that diamond powder inks with a large variety of particle sizes conducive to a wide variety of powder precursor porosities could be deposited onto substrates and densified in a CVD/CVI diamond reactor, and
2. to demonstrate that the processes of printing and densification could be repeated to iteratively build thick diamond deposits.

Developing specific formulations for high resolution printing was beyond the scope of this study.

Inks which contain submicrometer-sized particles yield low porosity precursors. Benzyl alcohol is an essential ingredient in preparations containing submicrometer-sized diamond particles. Benzyl alcohol appears to wet fine diamond powder and inhibit aggregation. Ultrafine diamond particles tend to aggregate when they are mixed with proprietary thinners such as Dupont 7480 and the proprietary Zyp Inc. vehicle and generic ethyl cellulose plus alpha terpineol preparations. Adding benzyl alcohol to these liquids reduces aggregation problems.

In addition to inhibiting aggregation, benzyl alcohol is a desirable liquid for adjusting ink viscosity because it evaporates slowly at room temperature, producing ink with a long "pot" life. Unfortunately, the rheological properties of inks that only contain benzyl alcohol plus diamond powder leave much to be desired with regard to pattern resolution. After drying, these precursors are soft and do not adhere strongly to substrates. Softness and poor adhesion limit opportunities for mechanically tailoring the powder precursors before densification.

A diamond ink with benzyl alcohol, plus a generic or the proprietary vehicle is superior to ink prepared simply from diamond powder plus benzyl alcohol. Dry powder green bodies prepared using the generic or proprietary vehicles are sufficiently robust to survive mechanical contouring, smoothing or thinning after drying. Additional powder layers can

be printed directly on these strong, dry deposits. The multicomponent formulations display improved rheological properties compatible with improved pattern resolution. Printing and painting techniques are suitable for forming diamond precursors that exceed 100  $\mu\text{m}$  in thickness with tailored porosities and surface topographies on selected areas.

## **II. Chemical Vapor Infiltration**

After representative porous diamond powder green bodies had dried, they were densified in the hot filament-assisted or the microwave plasma-assisted CVD/CVI reactors. When porous material is densified via chemical vapor infiltration, care must be taken, if possible, to avoid depositing a CVD “skin” that seals exterior pores and blocks densification of subsurface material. The porosity and thickness of a diamond precursor strongly affect whether the powder precursor will “skin over” before sufficient diamond has grown around interior particles to yield a mechanically strong, dense structure. Reactor conditions also strongly affect whether a dense surface skin forms before underlying pores are filled. In principle, in order to achieve complete densification, reactor conditions must be adjusted (if possible) so that the growth rate at the interior film/substrate interface exceeds the growth rate at the exterior surface.

### **A. Hot Filament-Assisted Reactor Results**

#### 1. General considerations

There are several phenomena which are known to occur during hot filament-assisted diamond deposition. In general, in hot filament-assisted reactors, CVD growth rate increases with working gas pressure when substrate temperature and the inlet molar concentration of the volatile carbon compound are held constant. Diamond growth rate depends on reactor geometry and can be maximized by adjusting substrate temperature, in combination with volatile carbon compound concentration and working gas pressure. Gas pressure cannot be increased towards the interior of a powder precursor. The atomic hydrogen vs volatile carbon compound concentration may vary across a powder precursor cross-section, but it is difficult to predict and control this variation. The deposition parameter that can most easily be controlled to tailor interior densification is substrate temperature. It is generally observed that CVD diamond grows faster with increasing substrate temperatures up to some maximum temperature between 900 to 1100 °C (depending on gas concentration, pressure and, perhaps, subtle reactor differences that are not well characterized by different groups doing diamond research). Above this maximum temperature, graphite forms relatively rapidly at the expense of diamond. Ideally, when densifying a powder precursor, one would wish to establish a temperature differential

across the precursor cross-section so the interior interface is at the optimal temperature for rapid diamond growth while the exterior of the precursor is somewhat cooler so good quality diamond grows more slowly. The temperature cross-section across a diamond deposit will be determined by the filament temperature, size and spacing, vs the temperature of the substrate heater. The properties of the diamond deposit being formed, e.g. surface emissivity, surface area, grain size and porosity may also affect temperature profile.

## 2. Preliminary results

After six hours in the reactor, 300  $\mu\text{m}$  thick, screen printed, high density green bodies on silicon substrates densify sufficiently so that they have potentially useful mechanical strength (Figure 3). These densified coatings survive aggressive scraping with screw drivers and dental probes. Similar deposits formed on nickel substrates (where graphite catalytically forms on the metal surface and serves as a release layer) have sufficient mechanical strength that allows free-standing pieces of diamond to be removed and handled. When subjected to similar treatment, porous green bodies with a narrow particle size distribution tend to fracture and crumble to reveal soft, powdery interiors.

Raman spectroscopy indicated that these densified composites contain good quality diamond. The best quality material, with the highest intensity, narrow Raman band at 1330  $\text{cm}^{-1}$  ( $\text{sp}^3$  bonded diamond) relative to a broad band at 1550  $\text{cm}^{-1}$  (amorphous and/or glassy carbon) occurs for material deposited using 0.5% methane as compared to 1% or 2% methane. A similar relationship between diamond coating quality and working gas composition is typically observed by groups depositing hot filament-assisted or microwave plasma-assisted CVD diamond.<sup>9</sup> The diamond Raman band is most dominant for CVI material formed at lower substrate temperatures (700 °C - see Figure 4) as compared to the substrate temperatures where many groups report observing their best quality CVD material (850 to 900 °C) for methane plus hydrogen gas chemistries.<sup>9</sup> The Raman spectrum of predominantly CVD diamond deposited on diamond-seeded 700 °C substrates in our reactor is similar to the spectrum of the 700 °C CVI material represented by Fig. 4A. However when marginal conditions for diamond deposition are present in our reactor, the CVI material contains a higher concentration of  $\text{sp}^3$  diamond bonds than the CVD material (compare Fig. 4B to 4C). The apparent “better quality” of the Raman spectra of the CVI material may not necessarily be due to better quality film deposited from the vapor phase. Because of finite sampling depth, Raman spectra for CVI materials have contributions from both the CVD deposited diamond and the precursor diamond powder. To give a more definitive statement, we would need to deconvolute the two components. Raman spectra

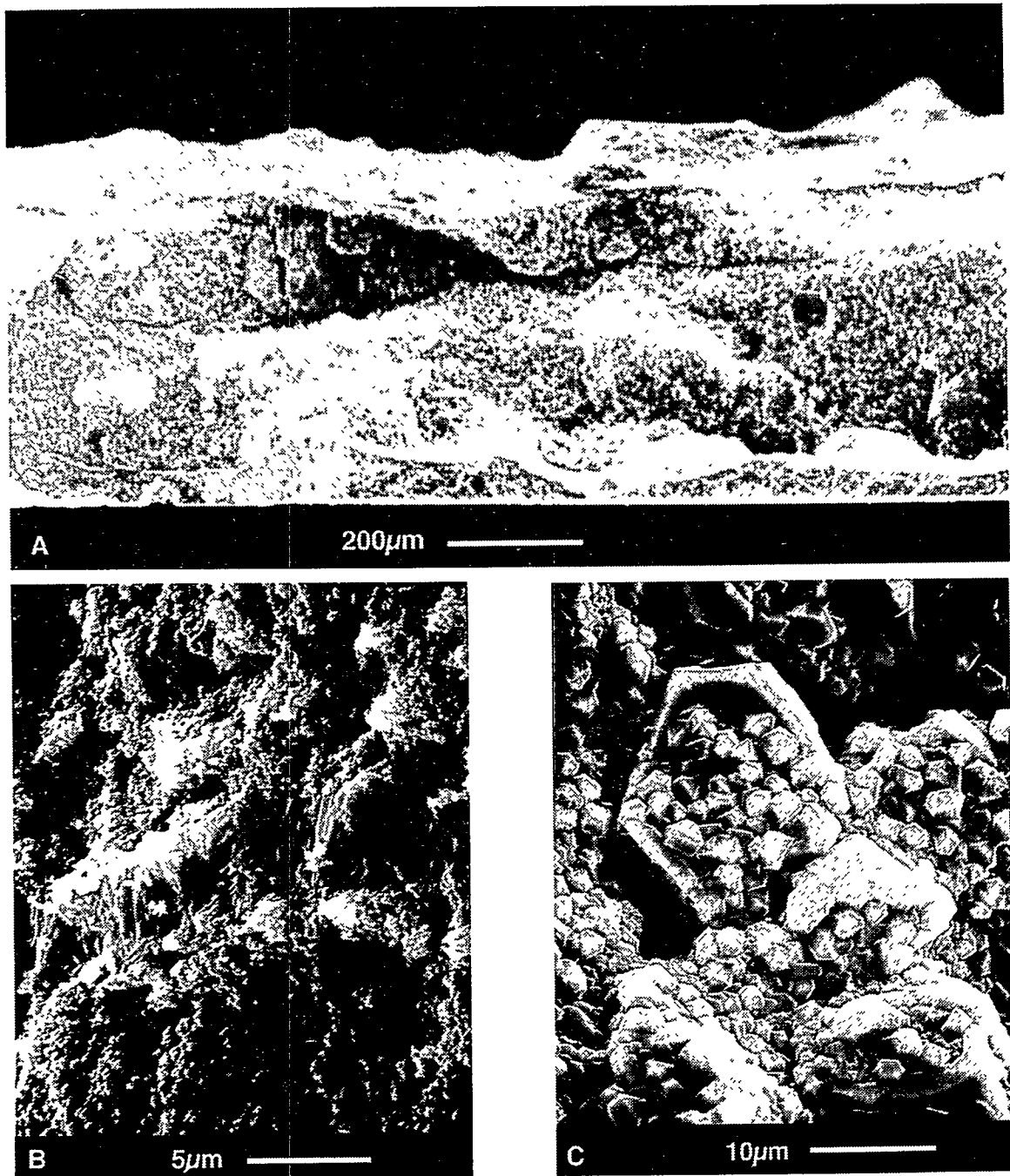


**Figure 3.** Densified, screen printed precursors. **A.** An extremely thick, 625  $\mu\text{m}$  deposit. **B.** Higher magnification view showing a buried CVI/CVD skin. **C.** Plan view of a partially densified powder deposit with faceted CVD diamond growth on surface diamond particles.

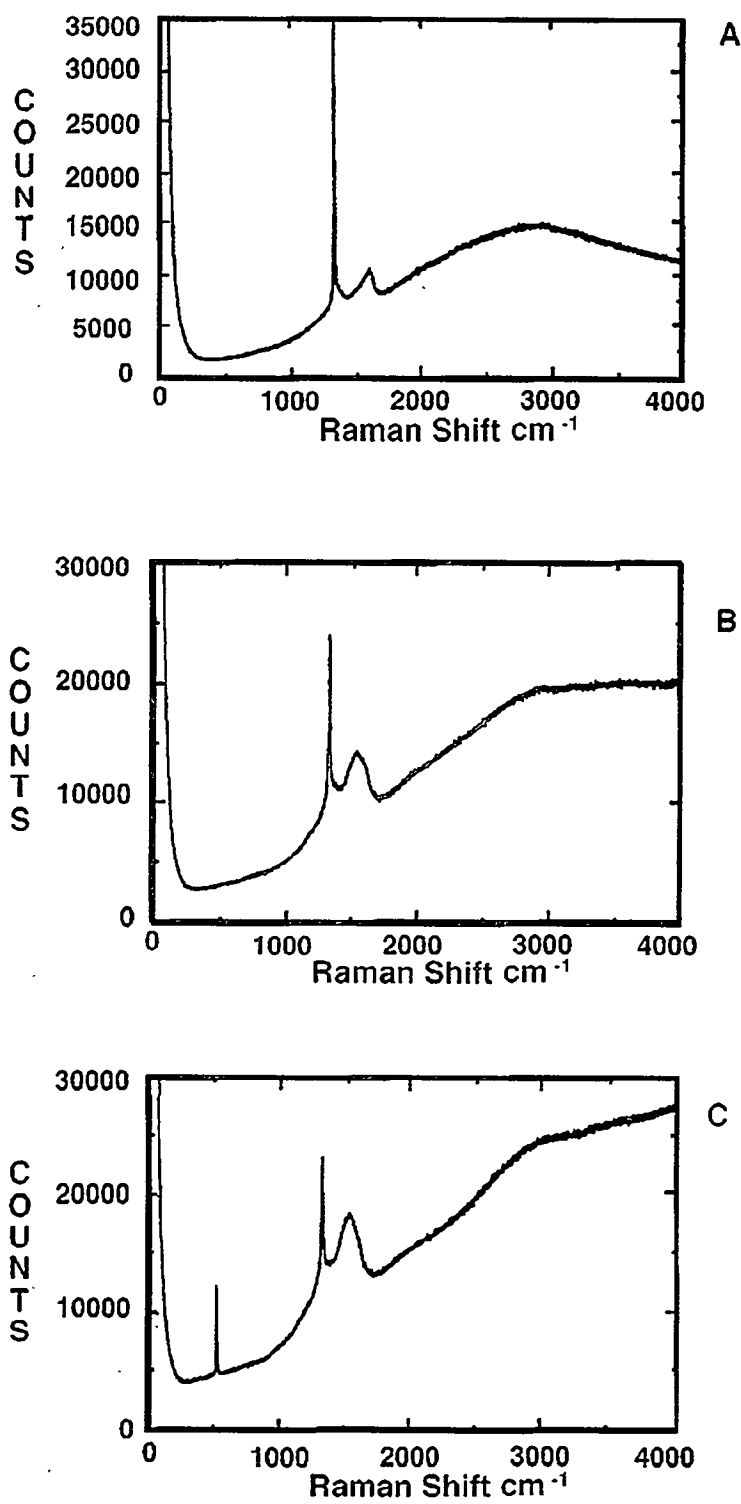


**Figure 4.** Raman spectra shifts. A. and B. From CVI densified screen printed diamond powder precursors processed at A. 700°C and B. 900°C CVI substrate temperatures. C. Predominantly CVD material formed at 900°C. (The 600  $\text{cm}^{-1}$  shift is silicon substrate shining through this relatively thin deposit.

displayed by densified, electrophoretically deposited precursors are similar to spectra displayed by screen printed deposits that were densified using similar substrate temperatures and methane concentrations.

The spectra from the CVI material contains fluorescence bands due to trace amounts of silicon and boron when boron doped silicon wafer substrates are used. Fluorescence bands due to silicon and boron entrainment are not present in the spectra of diamond composites formed on nickel substrates. The carbon bond Raman shifts exhibited by free-standing composites removed from nickel substrates are similar to those displayed by composite coatings formed on silicon.

Transmission electron microscopy indicates that the CVI diamond envelopes and enlarges interior diamond particles (Figure 5A and B). Diffraction patterns indicate the diamond composite material contains relatively few defects and little twinning (Figure 5C).

Plan view scanning electron micrographs of exterior surfaces of densified composites show a faceted topography with predominantly triangular (111) surface planes (Figure 5D and Figure 6). Larger surface grains form on composites densified at higher substrate temperatures. The exterior surface morphology of the composites is very similar to the surface morphology found on predominantly CVD material. This suggests that during the densification process, a CVD skin forms over the diamond powder green body. Thin buried CVD skins can be detected in extremely thick deposits formed by iteratively printing diamond ink then densifying (see Fig. 3B).

SEM micrographs (Fig. 7) indicate that, for certain process parameters, after twelve hours in the hot filament-assisted reactor, substantial amounts of chemically reactive vapor infiltrate through the diamond powder green body and deposit diamond at the interior surface (the surface originally touching the substrate). These micrographs corroborate Raman spectra which indicate significant amounts of carbon at the interior surface that has been deposited from the vapor phase (which includes some amount of diamond-like-carbon and glassy carbon - see Section 3 below). These micrographs corroborate qualitative observations that the interior surfaces of these free-standing pieces that have been treated in the reactor are mechanically robust and can survive aggressive scraping with a metal stylus. High density green bodies treated for only two to four hours in the hot filament assisted reactor and porous green bodies processed for twelve hours in the reactor are not

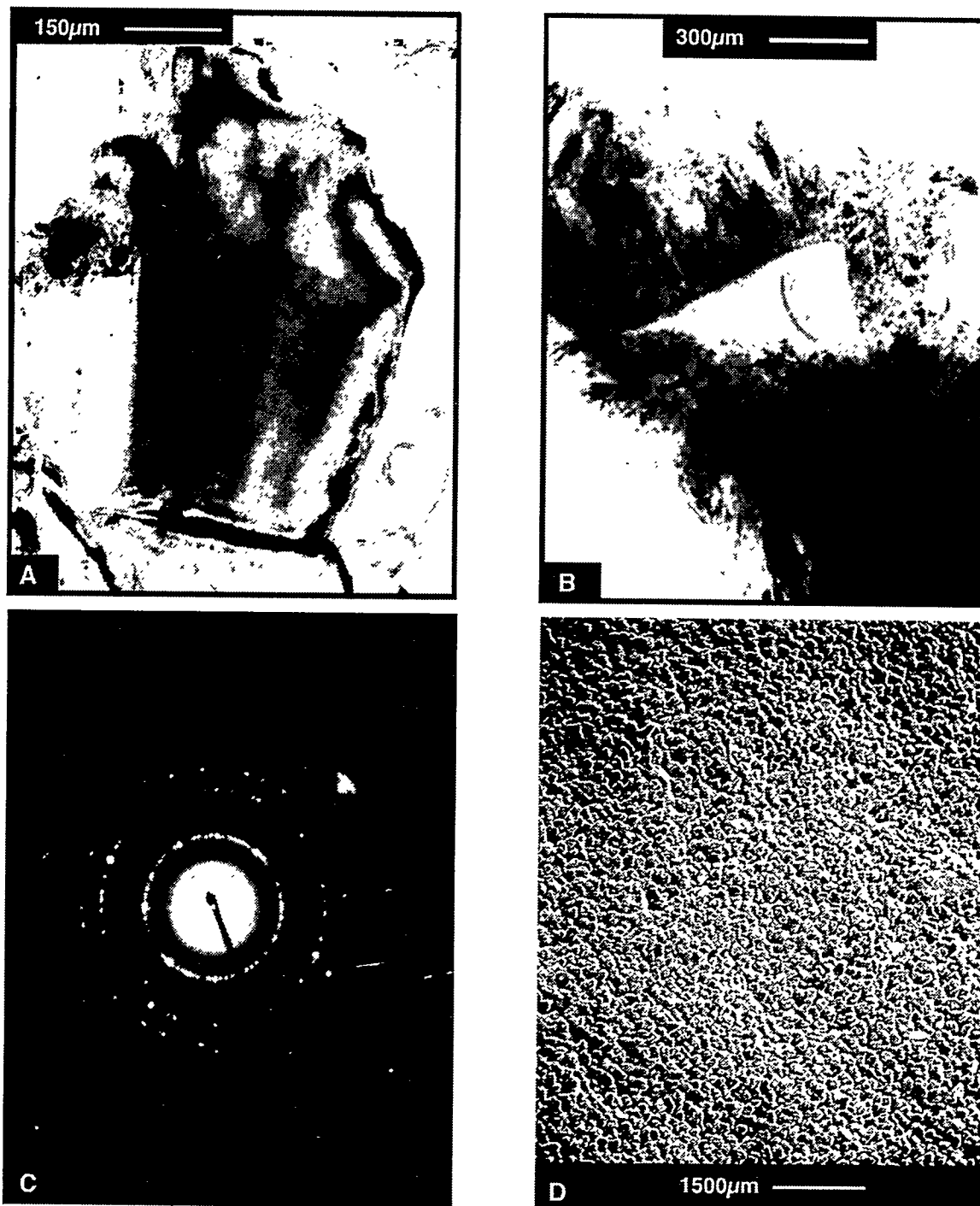


**Figure 5.** TEM and SEM analysis of CVI diamond deposits. **A.** Initial stage of densification. CVI material envelopes a diamond particle. **B.** As densification progresses, a thicker deposit grows around a particle. **C.** Electron diffraction pattern showing densified material has a well developed diamond structure. **D.** SEM plan view showing a faceted CVD diamond surface topography.

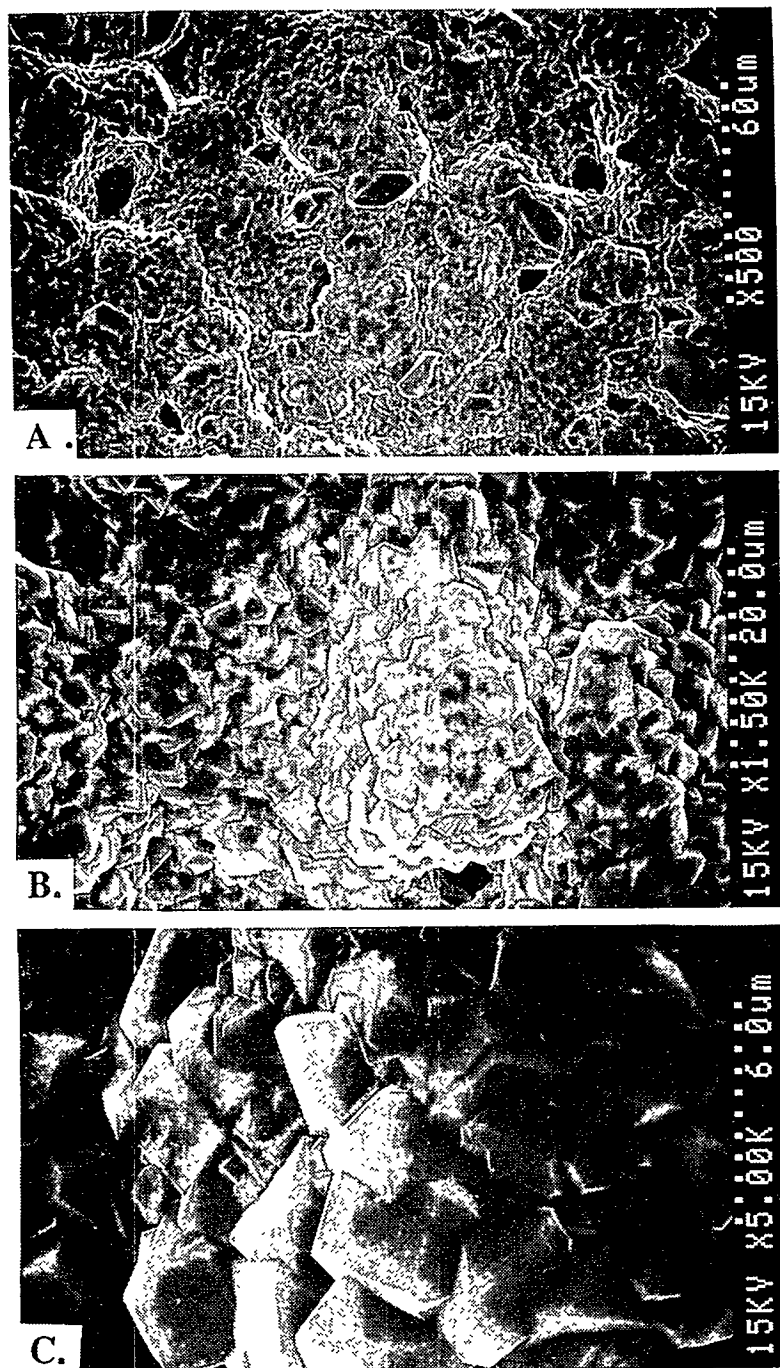


**Figure 6.** SEM micrographs of the exterior surface on the same filament-assisted reactor sample shown in Figure 7. **A.** Low magnification, **B.** Intermediate magnification and **C.** High magnification views. Even after 12 hours in the reactor, there are still pores in the surface that can feed additional densification at the interior.

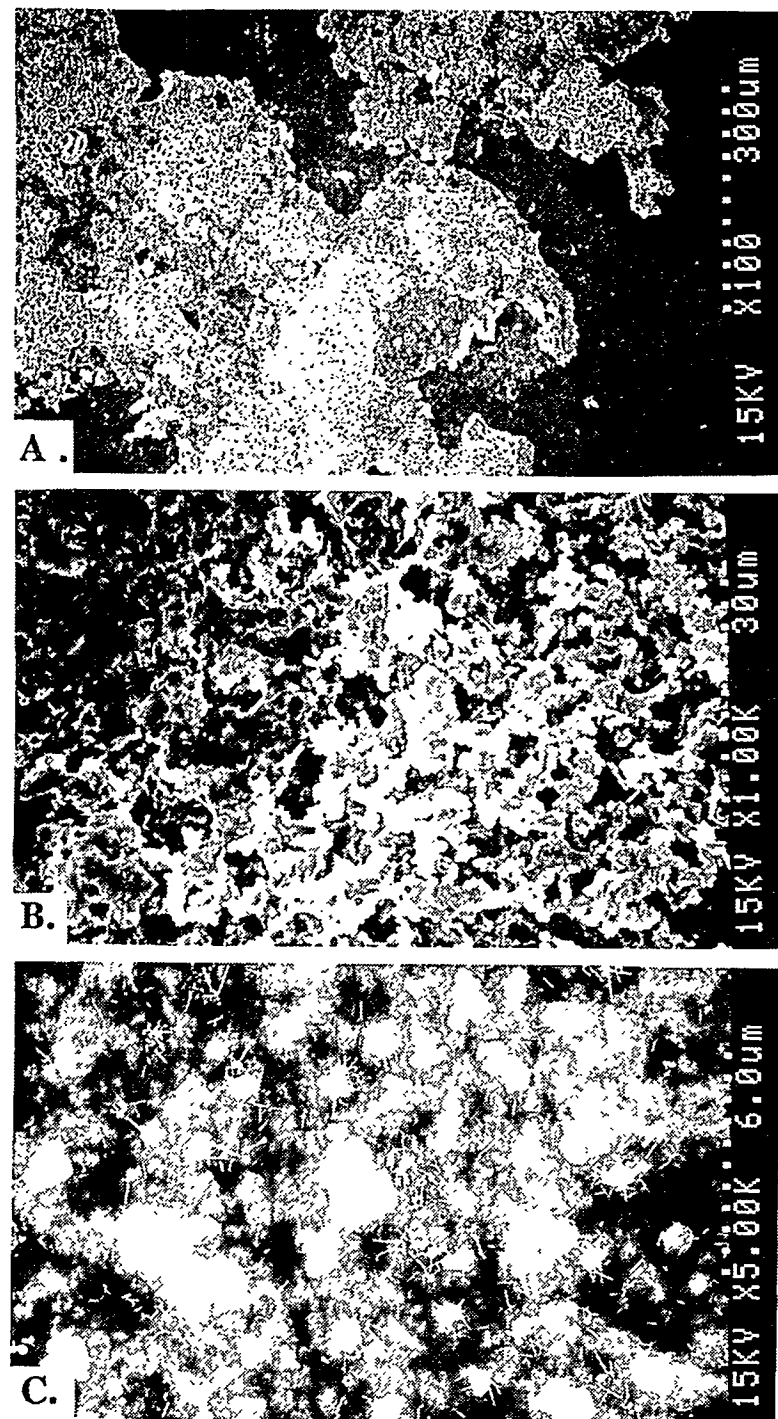


**Figure 7.** Scanning electron micrographs showing the interior surface of a free-standing hot filament-assisted CVI diamond/trimodal mix diamond powder composite. A 100  $\mu\text{m}$  thick diamond powder green body was placed in the reactor for 12 hr at 700  $^{\circ}\text{C}$  substrate temperature, 2200  $^{\circ}\text{C}$  filament temperature, 0.94 cm filament-substrate spacing, in 20 T. 0.5%  $\text{CH}_4$  plus hydrogen. **A.** Low magnification, **B.** Intermediate magnification and **C.** High magnification views. Significant amounts of CVI diamond have grown in the interior of the green body.

mechanically robust; there is some amount of free powder at the interior surface and the samples crumble when scraped with a stylus.

### 3. Fractional factorial designed experiments

Based on these preliminary experiments with the hot filament-assisted reactor, a second set of experimental parameter combinations were selected following a fractional factorial design with

- a. 10 or 20 Torr working gas pressure,
- b. 0.5 or 1% methane concentration in hydrogen,
- c. deposition times of 8 or 16 hours and
- d. substrate temperatures of 700 or 825 °C.

Patches of high density, 100 or 200  $\mu\text{m}$  thick diamond powder were screen printed on molybdenum substrates. These substrates also had patches that were abraded with diamond grit then wiped “clean” so that predominantly CVD diamond would form.

Micrographs of the exterior surface of representative samples showed microfaceted diamond growth with predominantly (111) surface planes and substantial amounts of twinning. Even after 16 hours in the hot filament-assisted reactor, the exterior material still had pores that could presumably feed vapor into the interior and support additional diamond growth there. Pores were also present in the interior material after 16 hours of reactor processing. No significant differences in the microstructure of any of the material produced by the fractional factorial experiments could be identified in the micrographs.

Raman spectroscopy indicated there are significant differences in the forms of carbon deposited by different fractional factorial-designed combinations of parameters. Figures 8, 9, and 10 show Raman spectra collected from

1. the exterior (outer) composite surface and
2. the interior (composite/substrate) surface of free standing diamond and
3. the exterior surface of predominantly CVD diamond coatings.

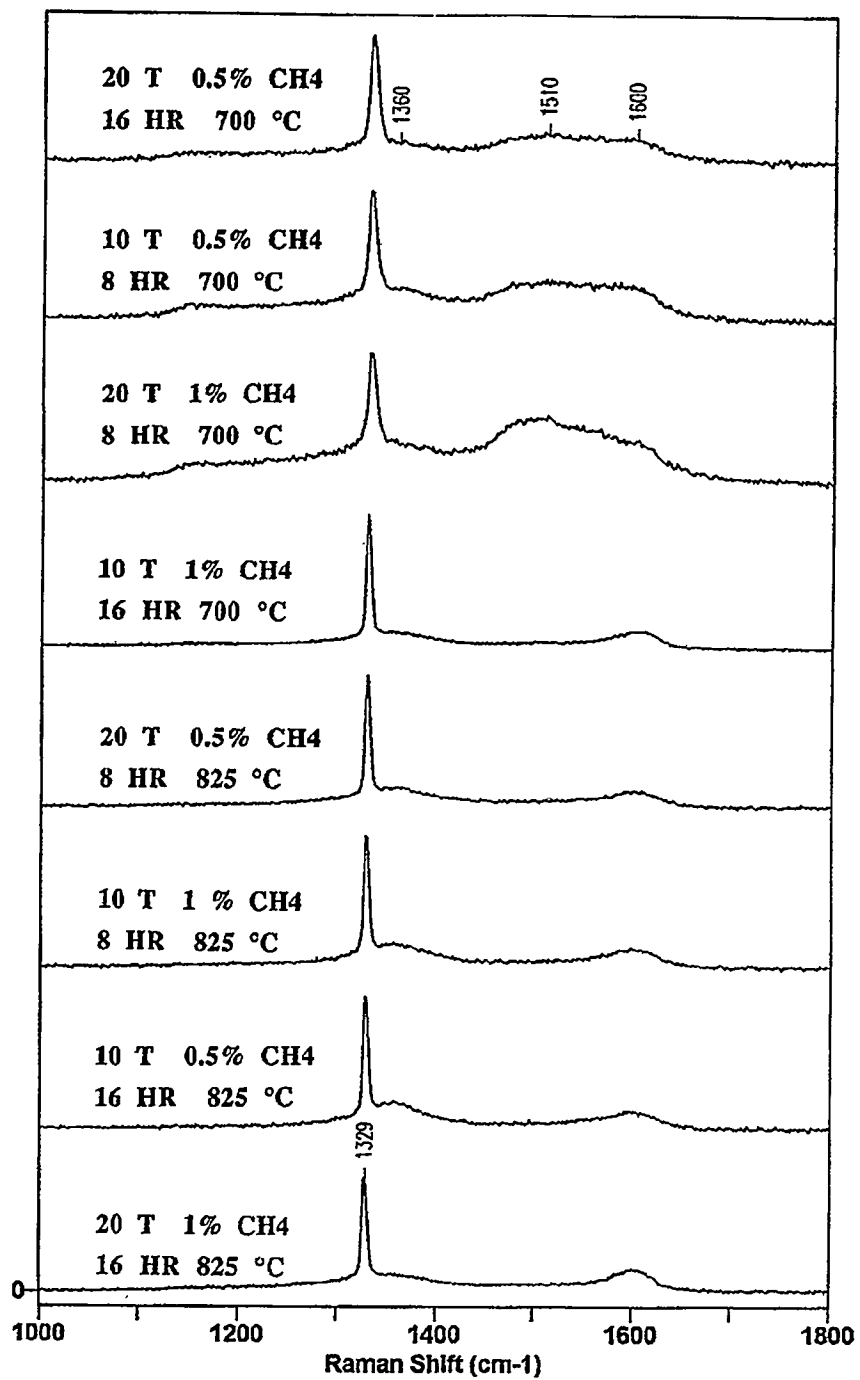


**Figure 8.** Raman spectra of the exterior surface of composites densified in the hot filament assisted-reactor following a fractional factorial experimental design.

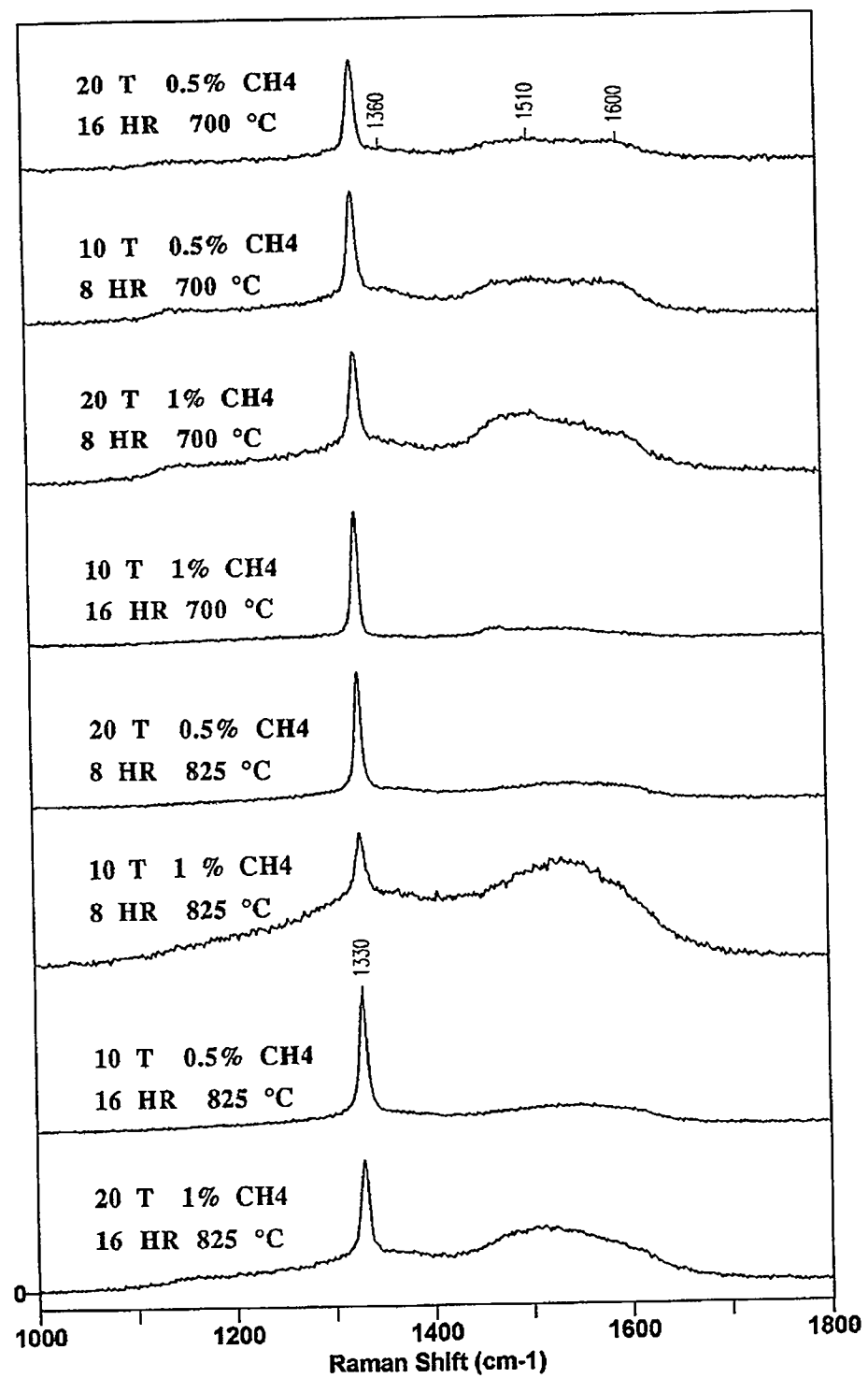


**Figure 9.** Raman spectra of the interior surface of free-standing composites densified in the hot filament-assisted reactor following a fractional factorial experimental design.

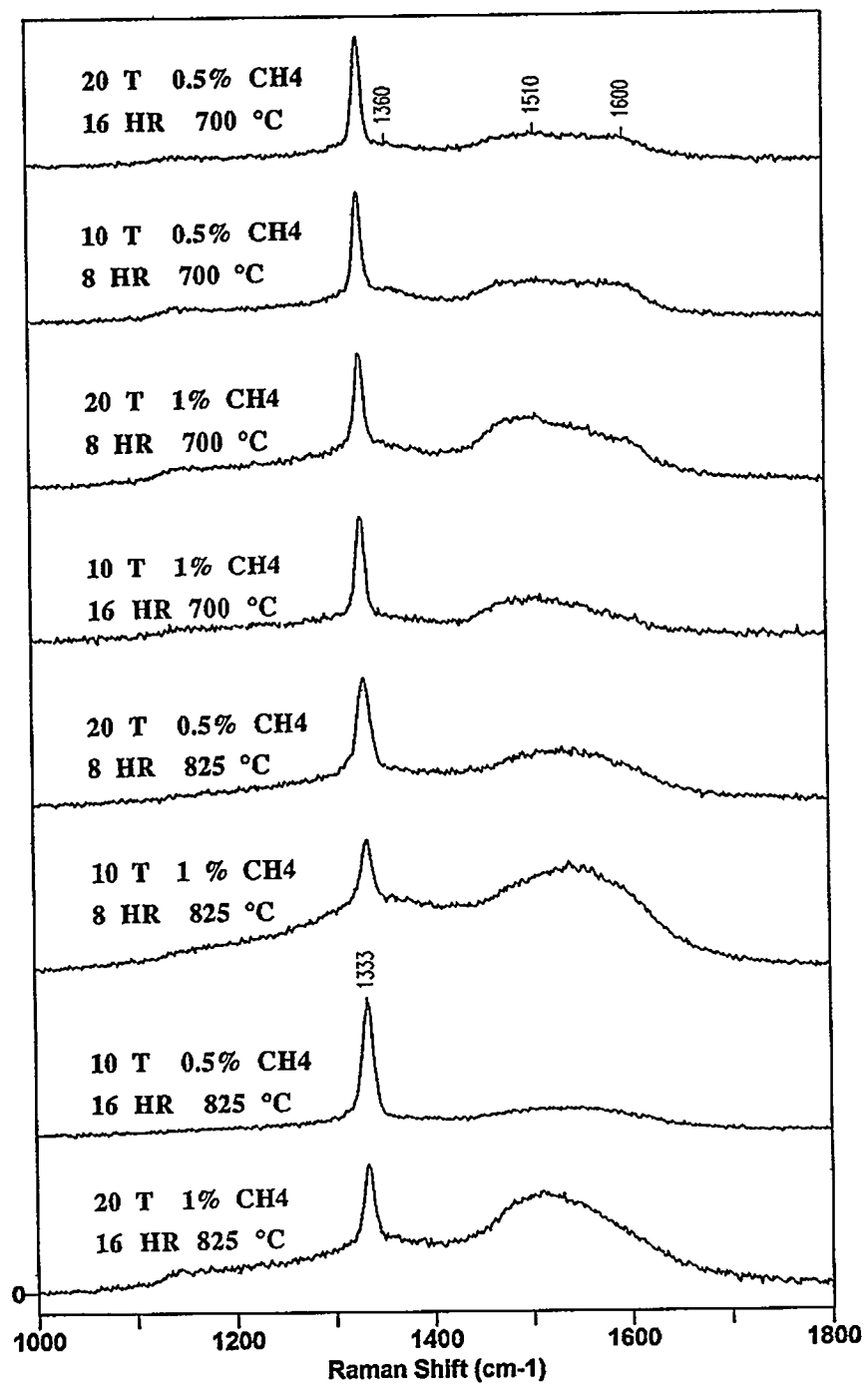


**Figure 10.** Raman spectra of the exterior surface of predominantly CVD coatings on molybdenum formed in the hot filament-assisted reactor following a fractional factorial experimental design.

Table 1 qualitatively interprets the Raman spectra and associated fluorescence spectra in terms of stress, composition, impurities and defects. These composites and coatings were formed using eight different combinations of (1) pressure, (2) methane concentration, (3) process time and (4) substrate temperature. A number of generalizations can be made:

- The mixture of carbon phases deposited on the exterior of the powder composites is different from the material deposited at the interior of the composites and predominantly CVD carbon. In addition to diamond, some of the composite exteriors contain glassy carbon ( $1600\text{ cm}^{-1}$ ). In addition to diamond, the composite interiors and predominantly CVD coating exteriors contain diamond-like-carbon ( $1500\text{ cm}^{-1}$ ). Some of the composite interiors also contain glassy carbon.
- The composite exteriors do not vary much as a function of the different combinations of processing conditions used. All have substantial amounts of diamond ( $\sim 1330\text{ cm}^{-1}$ ).
- With low methane concentrations (0.5%), at high substrate temperatures ( $825^\circ\text{C}$ ) relatively more diamond vs other forms of carbon is forming in the interior of the composites and on the predominantly CVD material.
- Pressure and process time do not have much of an effect on composition
- High substrate temperatures ( $825^\circ\text{C}$ ) in combination with high methane concentrations (1%) results in the lowest diamond to non-diamond carbon ratios for all three types of material analyzed: (1) composite exteriors (here the effect is smallest and temperature appears to be more important as compared to methane concentration.), (2) composite interiors and (3) the exterior surfaces of the predominantly CVD coatings.
- When processing conditions are marginal for optimal diamond growth, higher concentrations of diamond are present in the composite material as compared to the predominantly CVD material. There tends to be a lower incidence of observable compressive stress in the composites – especially at the composite exteriors. As noted above, the observation that better quality material is present in the composites may indicate (1) that better quality material is being deposited from the vapor phase and/or (2) that spectra originating from the high quality diamond powder are superimposed with spectra from overlying material deposited from the vapor phase.

Table 1  
HOT FILAMENT

		Carbon Forms (Raman)			Diamond-Phase Defects (Fluorescence)			
PROCESSING CONDITIONS	LOCATION	DIAMOND	DIAMOND WITH COMPRESSIVE STRESS	DIAMOND-LIKE CARBON	GLASSY CARBON	NITROGEN + vacancy	NICKEL doping + (Mo-defect?)	
10T 0.5% CH <sub>4</sub> 8 hr. 700 °C	CVD	X	X	X	X	X	X	
	CVI (interior)	X	X	X	X	X		
	CVI (exterior)	X	X	X	X	X		
20T 1% CH <sub>4</sub> 8 hr. 700 °C	CVD	X	X	X	X	X	X	
	CVI (interior)	X	X	X	X	X	X	
	CVI (exterior)	X	X	X	X	X		
20T 0.5% CH <sub>4</sub> 16 hr. 700 °C	CVD	X	X	X	X	X	X	
	CVI (interior)	X	X	X	X	X	X	
	CVI (exterior)	X	X	X	X	X		
10T 1% CH <sub>4</sub> 16 hr. 700 °C	CVD	X	X	X	X	X	X	
	CVI (interior)	X	X	X	X	X	X	
	CVI (exterior)	X	X	X	X	X		
20T 0.5% CH <sub>4</sub> 8 hr. 825 °C	CVD	X	X	X	X	X	X	
	CVI (interior)	X	X	X	X	X	X	
	CVI (exterior)	X	X	X	X	X		
10T 1% CH <sub>4</sub> 8 hr. 825 °C	CVD	X	X	X	X	X	X	
	CVI (interior)	X	X	X	X	X	X	
	CVI (exterior)	X	X	X	X	X		
10T 0.5% CH <sub>4</sub> 16 hr. 825 °C	CVD	X	X	X	X	X	X	
	CVI (interior)	X	X	X	X	X	X	
	CVI (exterior)	X	X	X	X	X		
20T 1% CH <sub>4</sub> 16 hr. 825 °C	CVD	X	X	X	X	X	X	
	CVI (interior)	X	X	X	X	X	X	
	CVI (exterior)	X	X	X	X	X		

## B. Microwave Plasma Assisted Reactor

### 1. General considerations

There are several phenomena which are known to occur during microwave plasma-assisted diamond deposition. In general, in a microwave plasma-assisted reactor, CVD growth rate increases with working gas pressure and power when substrate temperature and the percent concentration of the volatile carbon compound are held constant. Diamond growth rate is fastest at some optimal combination of substrate temperature and volatile carbon compound. Substrate temperature is strongly affected by the microwave fire ball. Because of the amount of heat generated by the fire ball, it was not necessary to ohmically heat substrates as aggressively in the microwave system as compared to the hot filament system to achieve a desired substrate temperature. Temperature differentials across composites treated in the microwave system were probably smaller than the temperature differentials in the hot filament system.

Atomic hydrogen is important to diamond growth because it etches away non-diamond forms of carbon faster than it etches away diamond. Some argue that atomic hydrogen also helps reshape electronic states of reactive carbon radicals from hexagonal  $sp^2$  directions into tetrahedral  $sp^3$  directions, more favorable for diamond growth. Chemically reactive carbon radicals such as  $CH_3$  are important as a raw material supporting coating growth. For the conditions used for this study (1% or less methane or methyl fluoride concentrations) the conversion efficiency from molecular hydrogen to atomic hydrogen in the microwave reactor and the hot filament system are probably similar. The conversion efficiency from methane to reactive  $CH_3$  radicals (and probably methyl fluoride to reactive radicals) roughly scale, so there are approximately similar ratios of reactive carbon radicals to atomic hydrogen present in both the microwave system as compared to the hot filament system. For the conditions studied, the concentration of methane to hydrogen (0.5 to 1%) that yields good quality diamond is similar for both types of reactor.

In a microwave plasma-assisted reactor, ions accelerate from the plasma across a ~50 to 100 V plasma sheath that surrounds grounded surfaces and bombard those surfaces. We initially hoped this ion bombardment might sputter away surface material, slow surface growth rate relative to the interior growth rate and promote composite densification. The micrographs presented below show this beneficial effect is not, in fact, contributing significantly, and skin formation in the microwave-assisted occurs far more rapidly as compared to the hot filament-assisted reactor. This may be a result of some difference in the temperature profile across the composites during processing as noted above.

## 2. Fractional factorial designed experiments

Preliminary experiments indicated variations of combinations of four parameters would be appropriate for a fractional factorial statistically designed experiment:

1. power and pressure: 0.9 KW and 20 T or 1.5 KW and 50 T,
2. volatile carbon compound: CH<sub>4</sub> or CH<sub>3</sub>F,
3. concentration: 0.5% or 1% in hydrogen and
4. substrate temperature: 700 or 825 °C.

All of the samples produced over the range of experimental conditions explored appeared to be somewhat similar when examined with optical and scanning electron microscopes. The amount of material deposited at the interior of diamond green bodies densified in a microwave plasma-assisted reactor is somewhat less than the amount deposited in a hot filament-assisted reactor. (Compare Figures 7C and 11D.) The exterior surfaces of composites formed in the microwave plasma-assisted reactor and the hot filament-assisted reactor appeared to be very similar except a more or less continuous skin was present on composites from microwave plasma-assisted reactor, while the skins on the hot filament-assisted reactor composites had pores. (Compare Figure 6A with Figure 11A.) High density green bodies made with a trimodal mixture of diamond powder sizes densified more readily than more porous green bodies with a narrow distribution of particle sizes. (Compare Figures 11 and 12.)

### a. Methane plus hydrogen experiments

Raman spectroscopy revealed significant differences between the fractional factorial samples. Figures 13, 14 and 15 and Table 2 show spectra and associated data interpretation. With regard to material formed using methane plus hydrogen the following generalizations can be made:

- For all experimental parameter combinations except the high power and pressure, low methane concentration, low temperature run, the CVI material is significantly better than the CVD material with regard to diamond concentration.

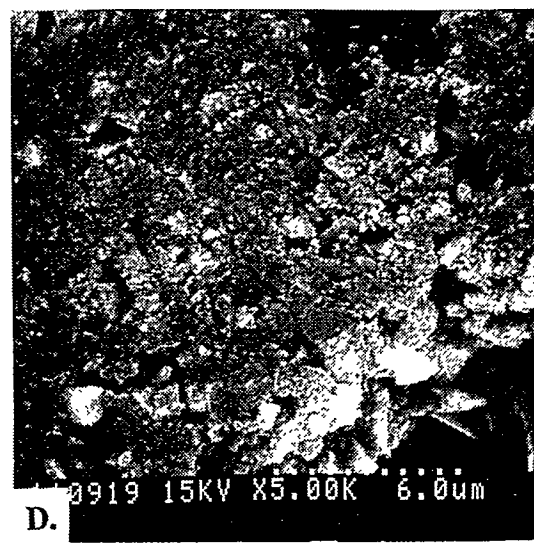
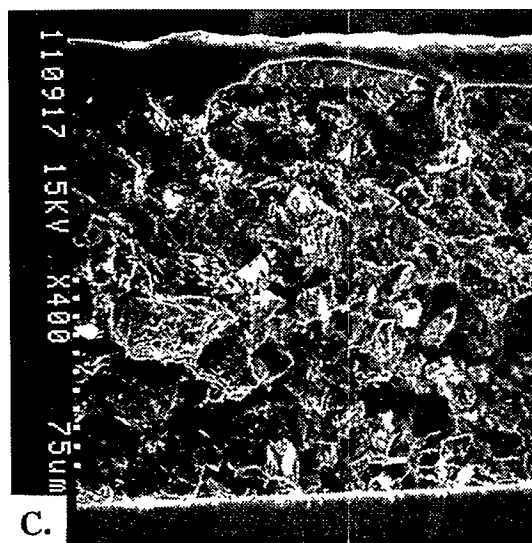
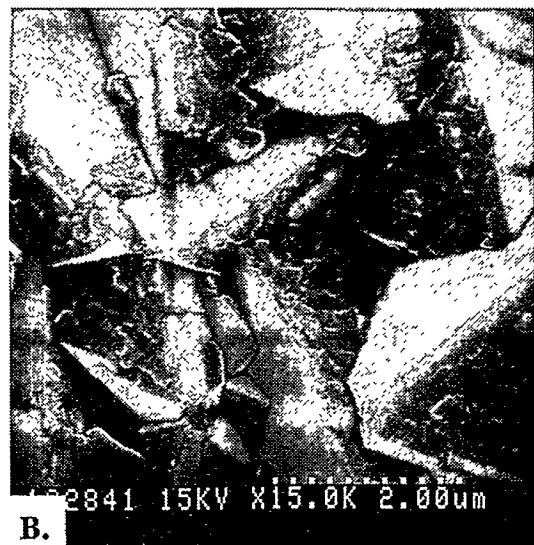
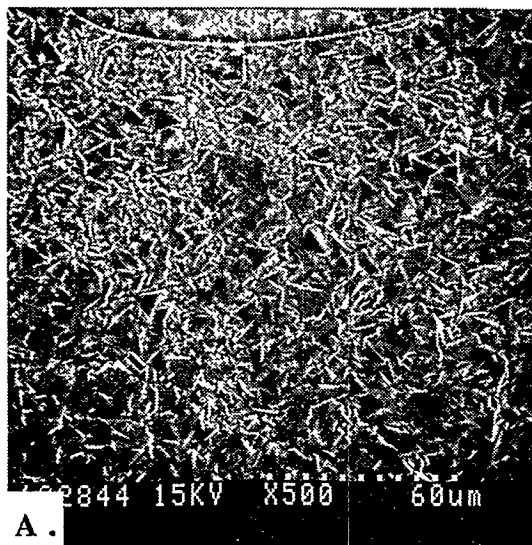


**Figure 11.** SEM micrographs showing a 100  $\mu\text{m}$  thick, high density (trimodal powder mix) diamond green body treated in the microwave plasma-assisted reactor: 900  $^{\circ}\text{C}$  substrate temperature, 1500 W, 50 T, 0.5% of  $\text{CH}_4$  plus hydrogen, 22 hours. **A.** Exterior surface, low magnification, **B.** Exterior Surface, high magnification, **C.** Cross-section, **D.** Interior surface. The exterior surface has “skinned over” before the interior surface has completely densified.

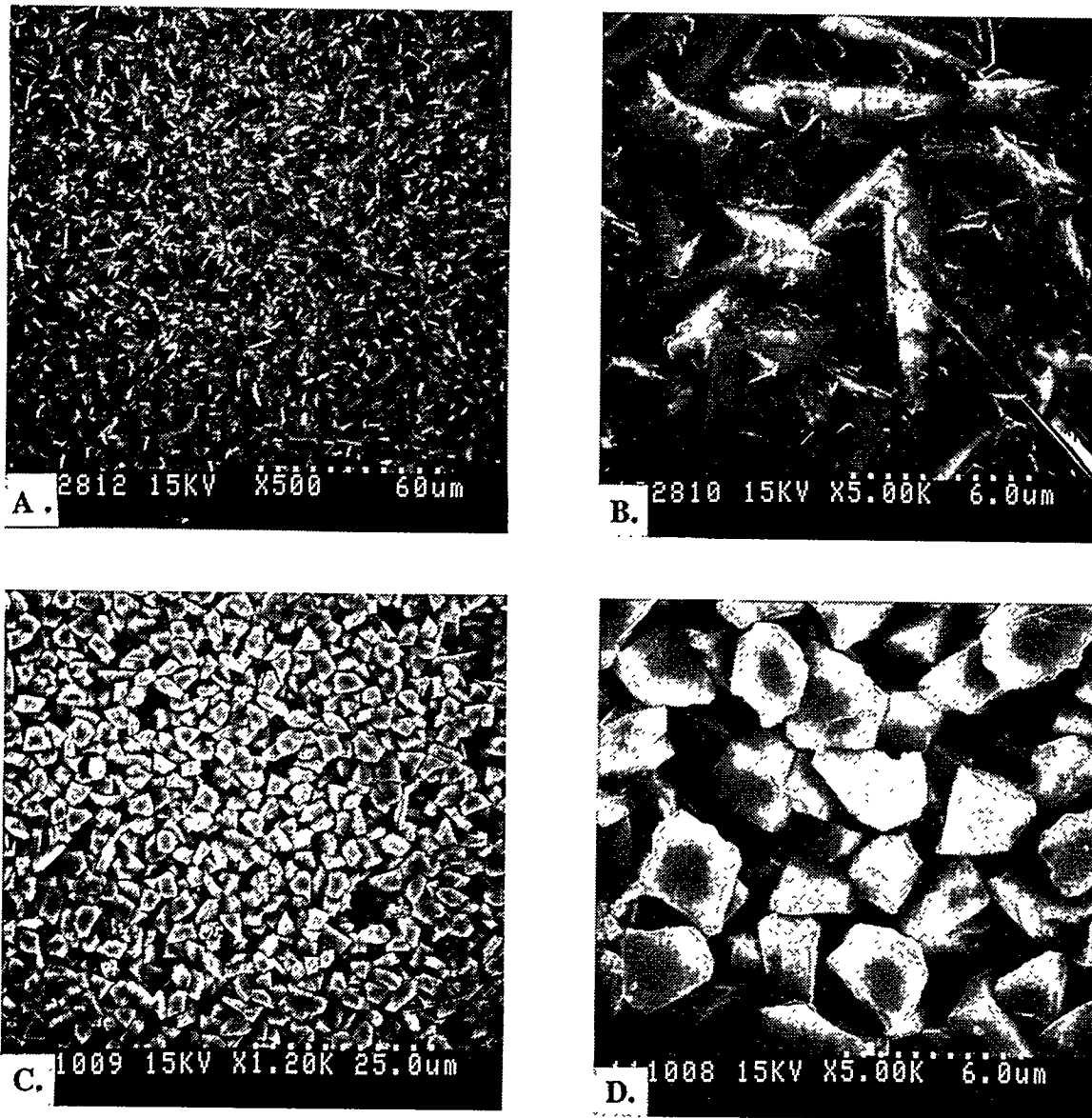


**Figure 12.** SEM micrographs of a 100  $\mu\text{m}$  thick, extremely porous diamond powder green body. (The green body was extremely porous because it was prepared from a narrow distribution of particle sizes, from 3 to 6  $\mu\text{m}$ .) This sample was treated in the microwave plasma-assisted reactor: 900  $^{\circ}\text{C}$  substrate temperature, 1500 W, 50 T, 0.5%  $\text{CH}_4$  plus hydrogen, 22 hours. **A.** Exterior surface, low magnification, **B.** Exterior surface, high magnification, **C.** Interior surface, low magnification, **D.** Interior surface, high magnification. The exterior surface has “skinned over.” The interior surface contains relatively little CVI material. The sample is extremely powdery and fragile.

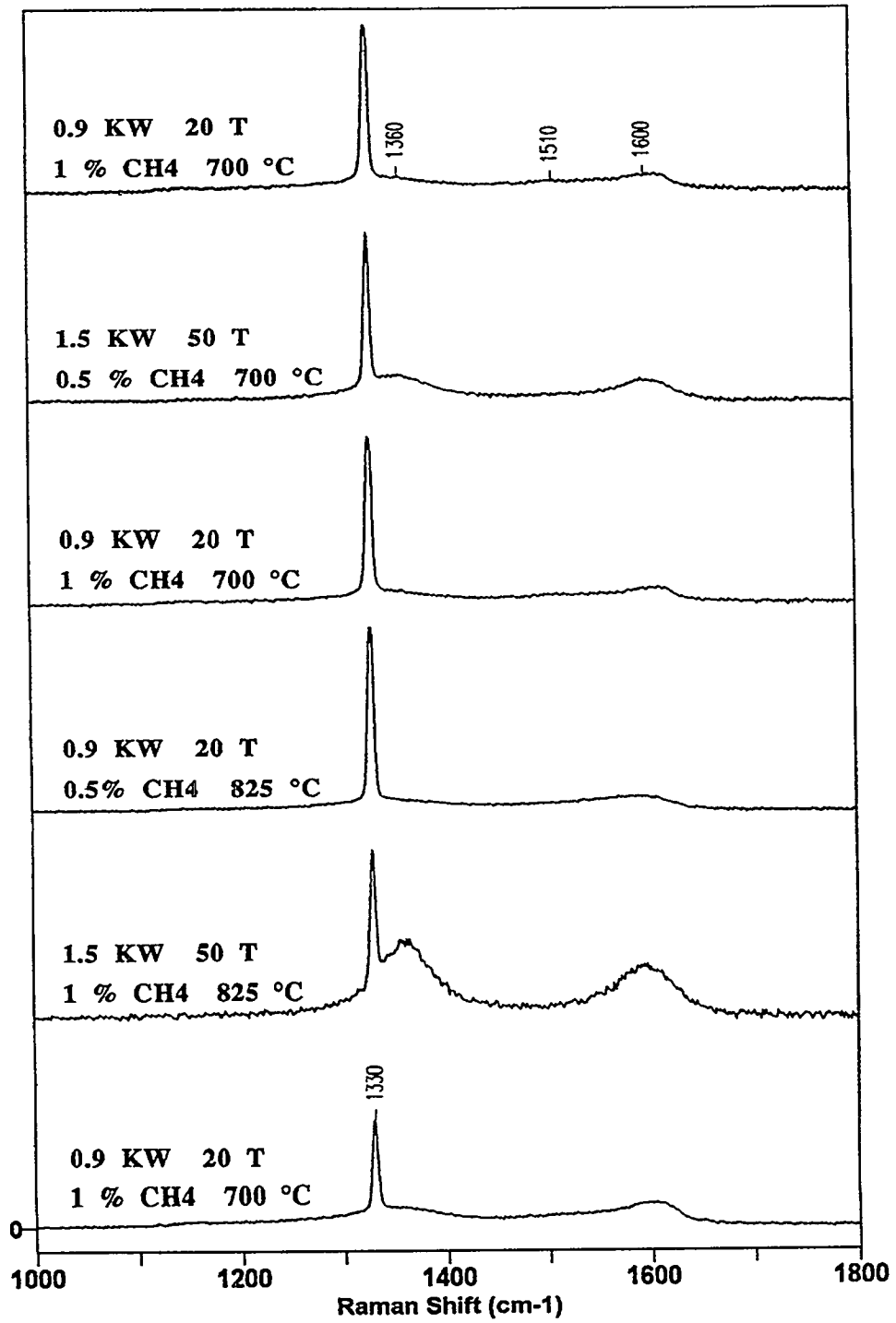


**Figure 13.** Raman spectra of the exterior surface of composites densified in the microwave plasma-assisted reactor following a fractional factorial experimental design with CH<sub>4</sub> plus hydrogen as the working gas.

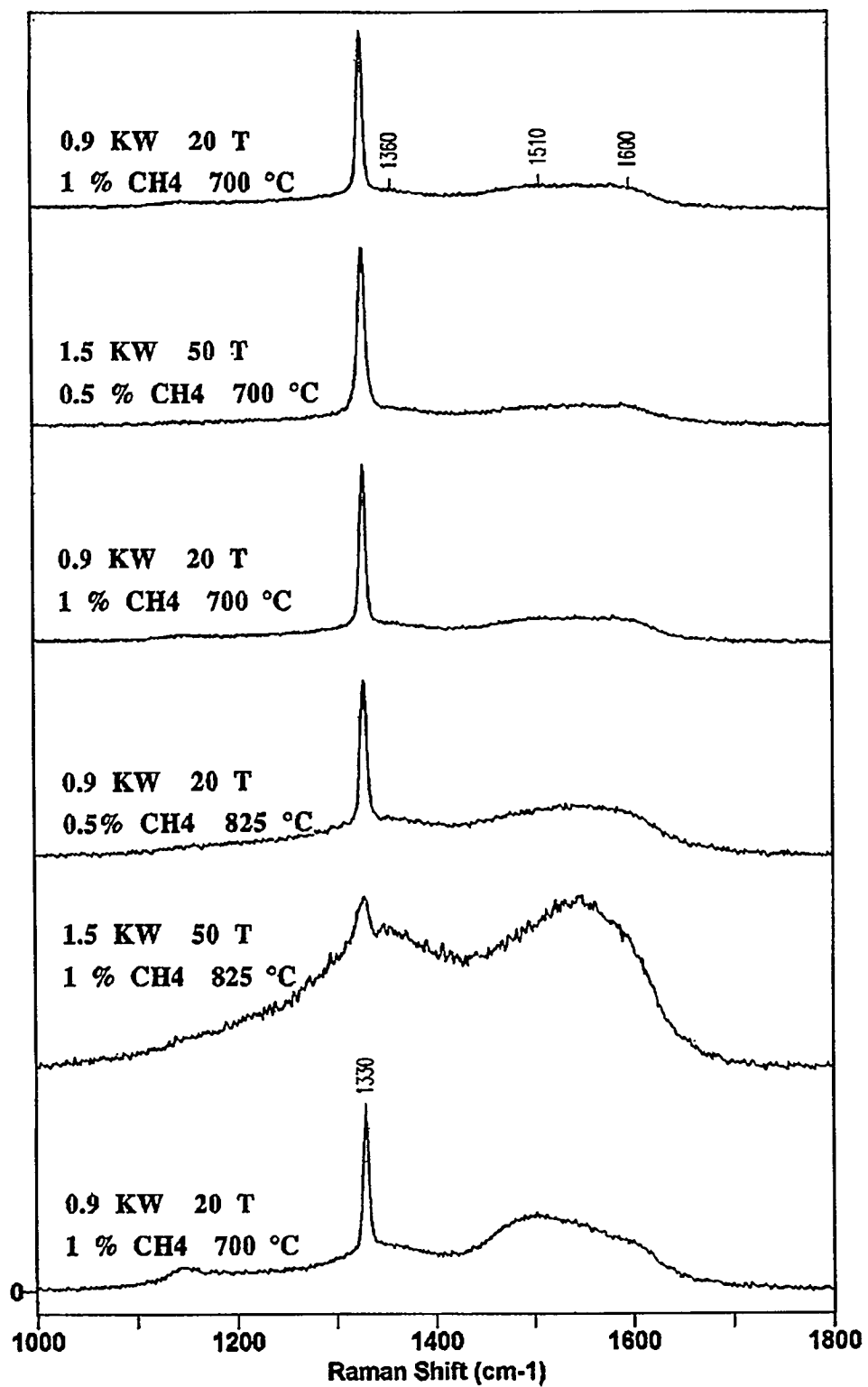


**Figure 14.** Raman spectra of the interior surface of free-standing composites densified in the microwave plasma-assisted reactor following a fractional factorial experimental design with  $\text{CH}_4$  plus hydrogen as the working gas.

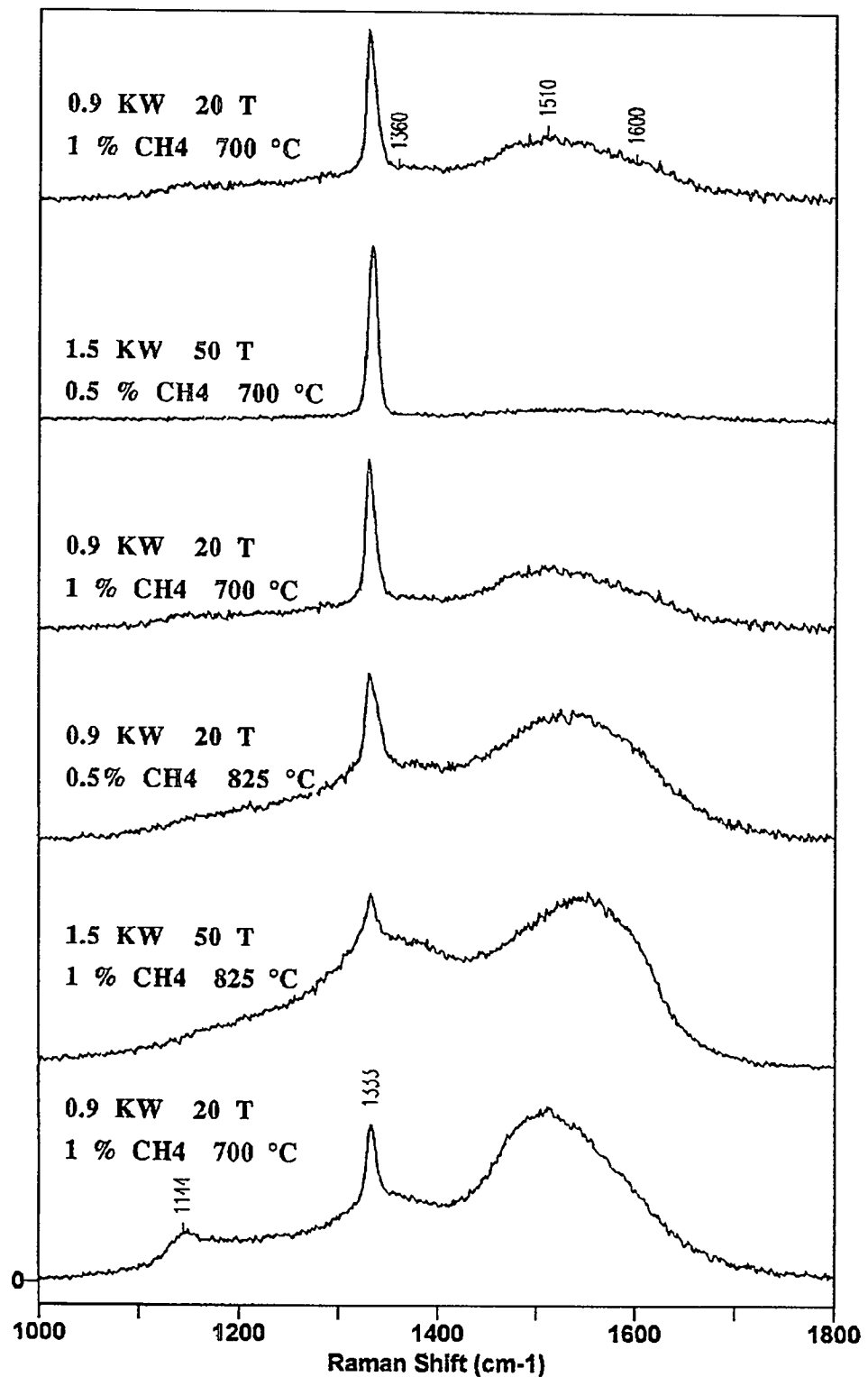


**Figure 15.** Raman spectra of predominantly CVD coatings on molybdenum substrates formed in the microwave plasma-assisted reactor following a fractional factorial experimental design with CH<sub>4</sub> plus hydrogen as the working gas.

Table 2

PROCESSING CONDITIONS	LOCATION	RAMAN BANDS			FLUORESCENCE		
		DIAMOND	DIAMOND WITH COMPRESSIVE STRESS	GLASSY CARBON	Nitrogen + Vacancy	Silicon	Nickel
1.5KW 50T 0.5% CH <sub>4</sub> 700 °C	CVD CVI (interior) CVI (exterior)	X	X	X	X	X	X
0.9KW 20T 1% CH <sub>4</sub> 700 °C	CVD CVI (interior) CVI (exterior)	X	X	X	X	X	X
0.9KW 20T 0.5% CH <sub>4</sub> 825 °C	CVD CVI (interior) CVI (exterior)	X	X	X	X	X	X
1.5KW 50T 1% CH <sub>4</sub> 825 °C	CVD CVI (interior) CVI (exterior)	X	X	X	X	X	X
0.9 KW 20T 1% CH <sub>4</sub> 700 °C	CVD CVI (interior) CVI (exterior)	X	X	X	X	X	X

- The interior of the densified powder samples and the predominantly CVD material contain diamond ( $\sim 1330 \text{ cm}^{-1}$ ), and some diamond-like-carbon ( $1500 - 1550 \text{ cm}^{-1}$ ), with a small amount of glassy carbon ( $\sim 1600 \text{ cm}^{-1}$ ) in a few samples. The exterior material on the powder samples consists of large amounts of diamond and some glassy carbon. (A similar spatial distribution of diamond, glassy carbon and diamond-like-carbon occurs for samples produced using the hot filament-assisted reactor.)
- In the CVI material, the highest diamond concentration vs other forms of carbon occurs in samples processed using low power/low pressure and low  $\text{CH}_4$  concentrations in combination with high substrate temperatures. The smallest diamond concentrations occur when high concentrations of methane and either all low or all high power, pressures and temperatures are combined.
- For the predominantly CVD material, the highest diamond concentrations are present in samples processed using high power/high pressure and low  $\text{CH}_4$  concentrations in combination with a low substrate temperature. The lowest diamond concentrations occur in conjunction with high values of all the parameters or low values of all the parameters.

In summary, high concentrations of diamond form when either low methane concentrations are used or low power/low pressure conditions are used. These conditions may affect the balance between the growth rate and nucleation rate of different carbon structures in some subtle way.

#### b. Methyl fluoride plus hydrogen experiments

Raman spectroscopy revealed smaller differences between material formed from methyl fluoride plus hydrogen compared to material produced using methane plus hydrogen over the parameter space evaluated. Figures 16, 17 and 18 and Table 3 show spectra and a qualitative interpretation of Raman and associated fluorescence data. With regard to material formed using methyl fluoride plus hydrogen the following generalizations can be made:

- Compared to the methane, methyl fluoride yields material with high concentrations of diamond over a broader range of conditions.

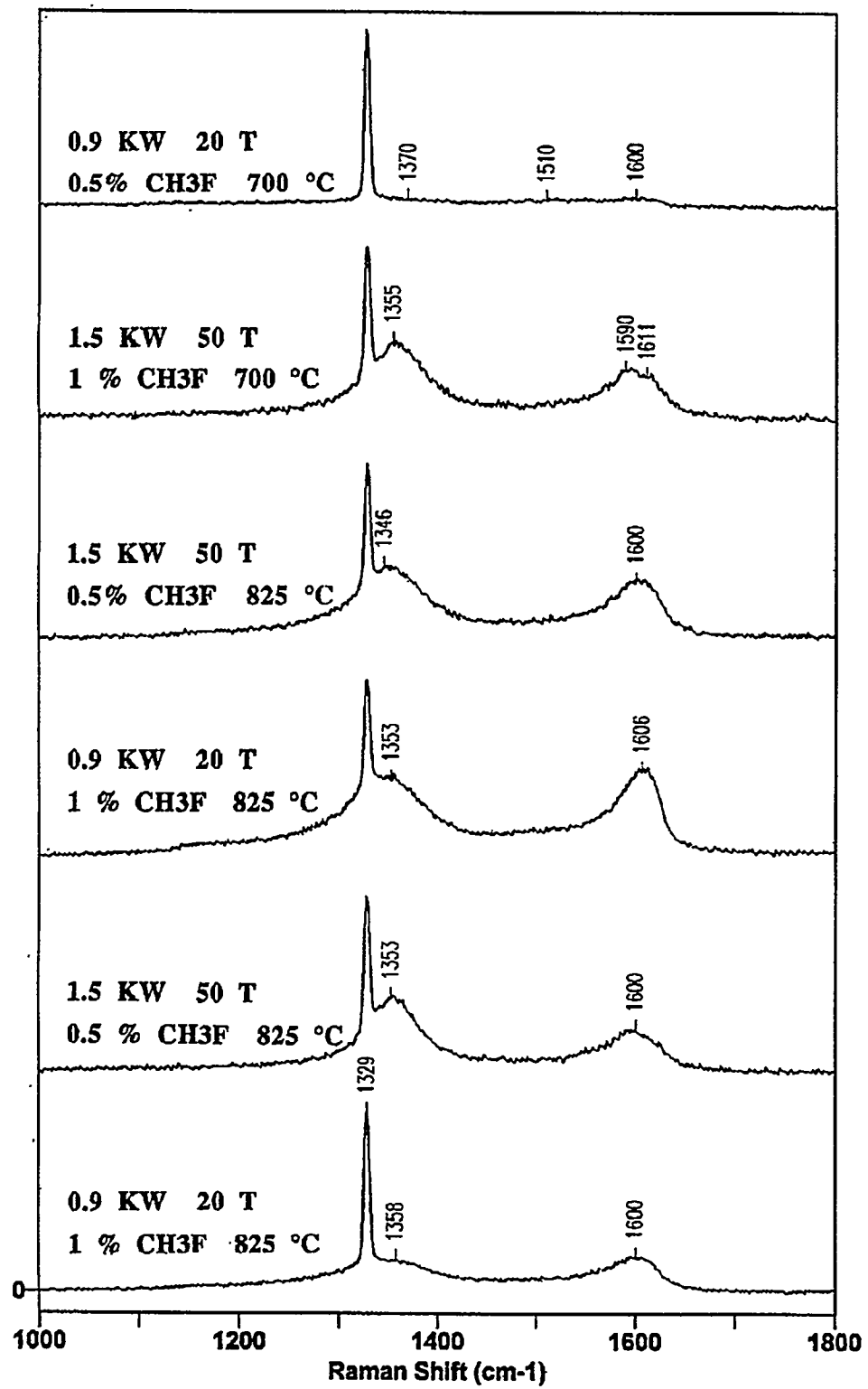


**Figure 16.** Raman spectra of the exterior surface of composites densified in the microwave plasma-assisted reactor following a fractional factorial experimental design with CH<sub>3</sub>F plus hydrogen as the working gas.

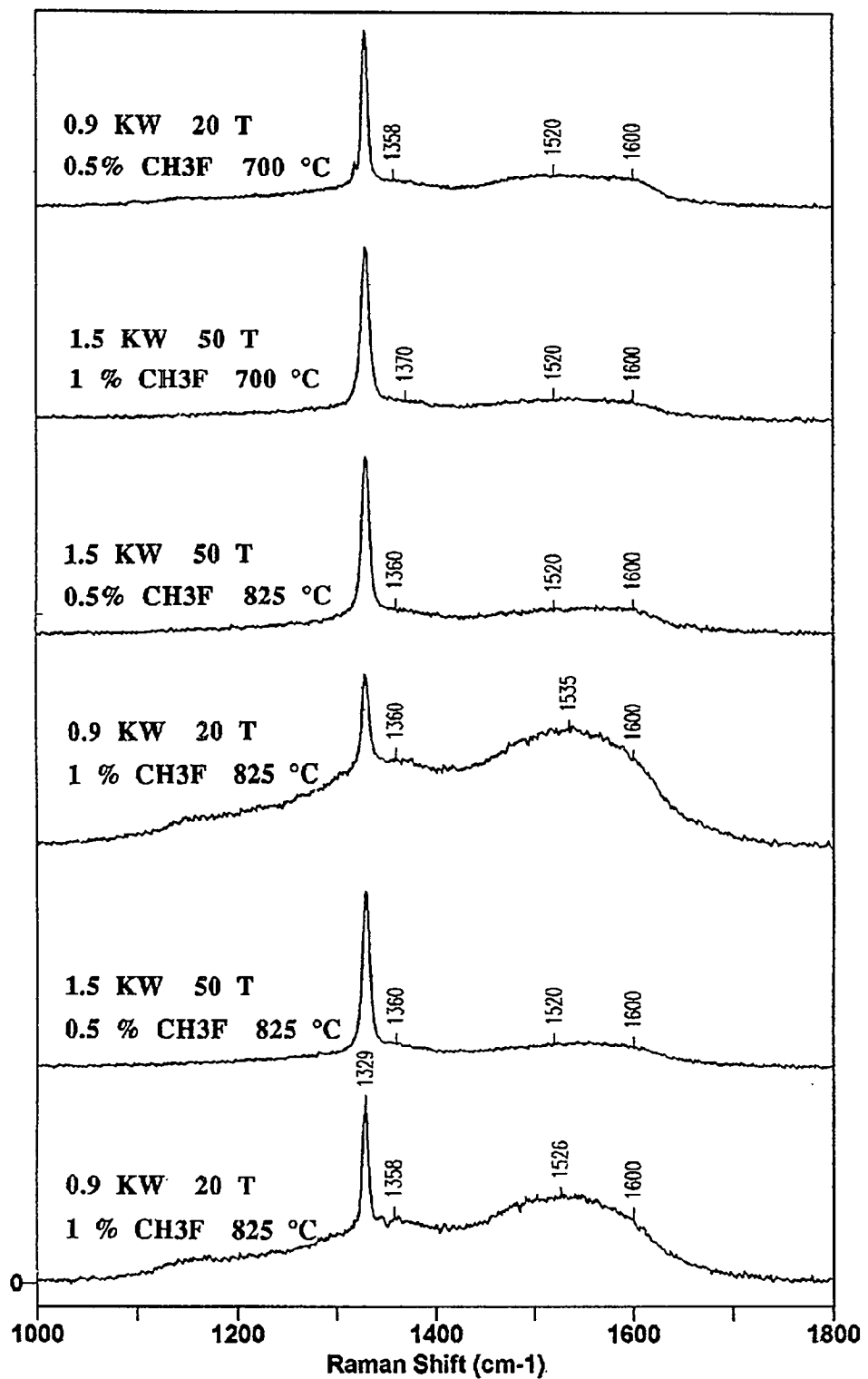


**Figure 17.** Raman spectra of the interior surface of free-standing composites densified in the microwave plasma-assisted reactor following a fractional factorial experimental design with CH<sub>3</sub>F plus hydrogen as the working gas.

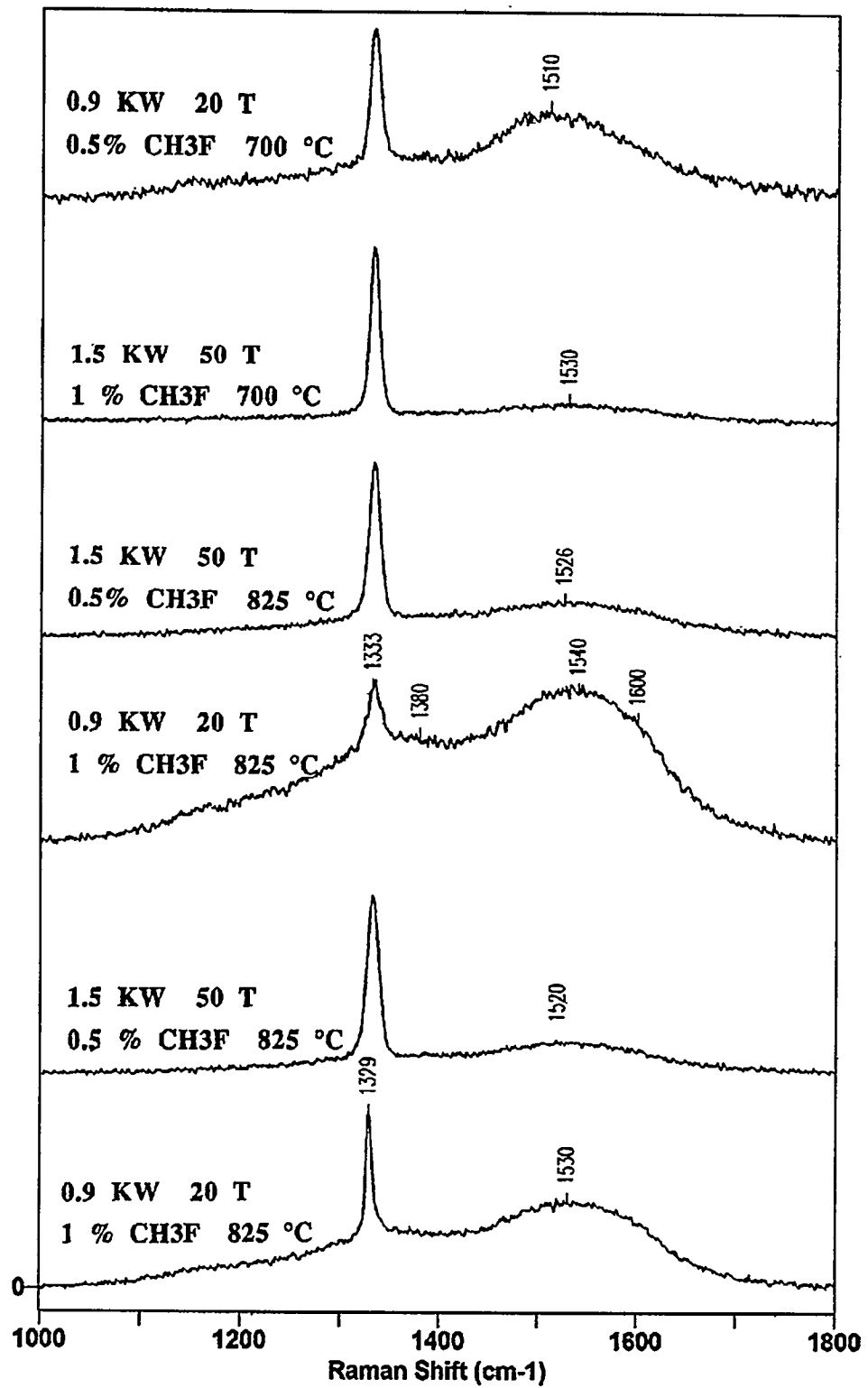


**Figure 18.** Raman spectra of predominantly CVD coatings on molybdenum substrates formed in the microwave plasma-assisted reactor following a fractional factorial experimental design with CH<sub>3</sub>F plus hydrogen as the working gas.

Table 3  
MICROWAVE

		Carbon Forms						Diamond-Phase Defects		
PROCESSING CONDITIONS	LOCATION	DIAMOND	DIAMOND WITH COMPRESSIVE STRESS	DIAMOND-LIKE CARBON	GLASSY CARBON	NITROGEN +	SILICON	NICKEL		
0.9KW 20T 0.5% CH <sub>3</sub> F 700 °C	CVD	X		X	X	X	X	X		
	CVI (interior)	X		X	X	X	X	X		
	CVI (exterior)	X		X	X	X	X	X		
1.5KW 50T 1% CH <sub>3</sub> F 700 °C	CVD	X		X	X	X	X	X		
	CVI (interior)	X		X	X	X	X	X		
	CVI (exterior)	X		X	X	X	X	X		
1.5KW 50T 0.5% CH <sub>3</sub> F 825 °C	CVD	X		X	X	X	X	X		
	CVI (interior)	X		X	X	X	X	X		
	CVI (exterior)	X		X	X	X	X	X		
0.9KW 20T 1% CH <sub>3</sub> F 825 °C	CVD	X		X	X	X	X	X		
	CVI (interior)	X		X	X	X	X	X		
	CVI (exterior)	X		X	X	X	X	X		
1.5KW 50T 0.5% CH <sub>3</sub> F 825 °C	CVD	X		X	X	X	X	X		
	CVI (interior)	X		X	X	X	X	X		
	CVI (exterior)	X		X	X	X	X	X		
0.9KW 20T 1% CH <sub>3</sub> F 825 °C	CVD	X		X	X	?	X	X		
	CVI (interior)	X		X	X	X	X	X		
	CVI (exterior)	X		X	X	X	X	X		

- There are smaller differences between the CVI material and the predominantly CVD material when methyl fluoride is used instead of methane.
- When methyl fluoride is used as a carbon source, the exterior of the CVI deposits contain large amounts of diamond mixed with some glassy carbon ( $1600\text{ cm}^{-1}$ ). The interior of the CVI samples and the predominantly CVD samples contain diamond plus some diamond-like-carbon, with a small amount of glassy carbon in some samples. (This is similar to the spatial distributions of carbon present in samples produced using methane in the hot filament-assisted and microwave plasma assisted reactors.)
- The smallest concentration of diamond occurs in samples formed using low power/low pressure plus high methyl fluoride concentrations.

## C. Additional Analysis

A limited number of representative samples that displayed strong,  $1331\text{ cm}^{-1}$  Raman shifts were submitted for additional analysis pertaining to optical transmittance, electron emissivity and electron beam excited fluorescence.

### 1. Optical transmittance

Good quality, natural diamond is transparent from the conduction band edge at an ultraviolet wavelength of approximately  $0.2\text{ }\mu\text{m}$  to the extremely far infrared (wavelengths of several hundreds of micrometers) with a relatively shallow lattice absorption at a wavelength centered around  $5\text{ }\mu\text{m}$ . Optical windows represent one of the most immediate practical applications for free-standing pieces of diamond.

Unfortunately, CVD diamond thicker than approximately  $1\text{ }\mu\text{m}$  tends to be grey because of flaws, twinning, and/or non-diamond carbon. Just trace amounts of absorbing material substantially detract from optical transmittance. The transmittance of our diamond composites is compromised by the presence of non-diamond carbon and scattering.

Figure 19 shows the amount of light reflected at visible wavelengths by polished silicon wafers without (experimental control) and with  $100\text{ }\mu\text{m}$  thick composite coatings before and after treatment in an oxygen tube furnace. Coatings with low transmittance have high absorptance. Relatively little light reflects from grey, high absorptance, as-deposited coatings on mirror-like silicon substrates (Fig. 19A). After these grey coatings are treated in an oxygen tube furnace for one hour at  $600\text{ }^{\circ}\text{C}$ , substantially more light reflects off the

coated silicon mirrors (Fig.19B). Less aggressive heat treatments (500 °C for four hours) result in relatively little increase in reflectivity (transmittivity). More aggressive heat treatments (700 °C for one hour) transform composites into dust.

Figure 20 shows the amount of light absorbed by silicon wafers that are polished on both sides, with a 100  $\mu\text{m}$  thick diamond composite on one side. This figure shows data collected at near-infrared wavelengths where silicon is relatively transparent. Figure 20 shows substantially more infrared light is transmitted through coated samples that have been treated at 600 °C for one hour in the oxygen tube furnace.

The increased transmittance/decreased absorptance that occurs as a result of the 600 °C/one hour oxygen treatment is readily visible. Before heat treatment, both sides of freestanding composites are grey. After treatment, both sides of composites formed in the hot filament-assisted reactor are white. On composites formed in the microwave plasma-assisted reactor, the surface exposed to oxygen flow becomes white while the under-surface remains grey (additional circumstantial evidence that a tight skin has formed on the microwave plasma assisted reactor samples while the hot filament assisted reactor samples have an open structure).

Burning-off non-diamond carbon (quantified by the Raman spectra shown in Figures 21 and 22) removes significant amounts of material (compare the micrographs of a treated sample in Figure 23 to an untreated sample – Figure 6). If this approach is pursued as a technique for forming thick transparent windows, then it is advisable to take an iterative approach of densifying powder composites in the reactor, then burning off the non-diamond carbon in the tube furnace, then returning the composite to the reactor to add more diamond plus non-diamond carbon and burning off the second batch of non-diamond carbon, . . . and so on.

## 2. Electron emissivity

CVD diamond, perhaps in combination with diamond-like-carbon and glassy carbon, is reported to have an extremely low work function or a negative electron affinity.<sup>10</sup> Published reports of this effect originate from only a few research groups. Although the origin of negative electron affinity in CVD diamond is not well understood, there is some speculation that negative electron affinity exists in films exhibiting predominantly hydrogen terminated (111) surface planes with some amount of non-diamond carbon (or in natural diamond, boron) acting as a dopant.

**OPTICAL REFLECTANCE**  
**FROM HOT FILAMENT CVI DIAMOND COATINGS**  
**ON SILICON SUBSTRATES**  
**(UV - VISIBLE)**

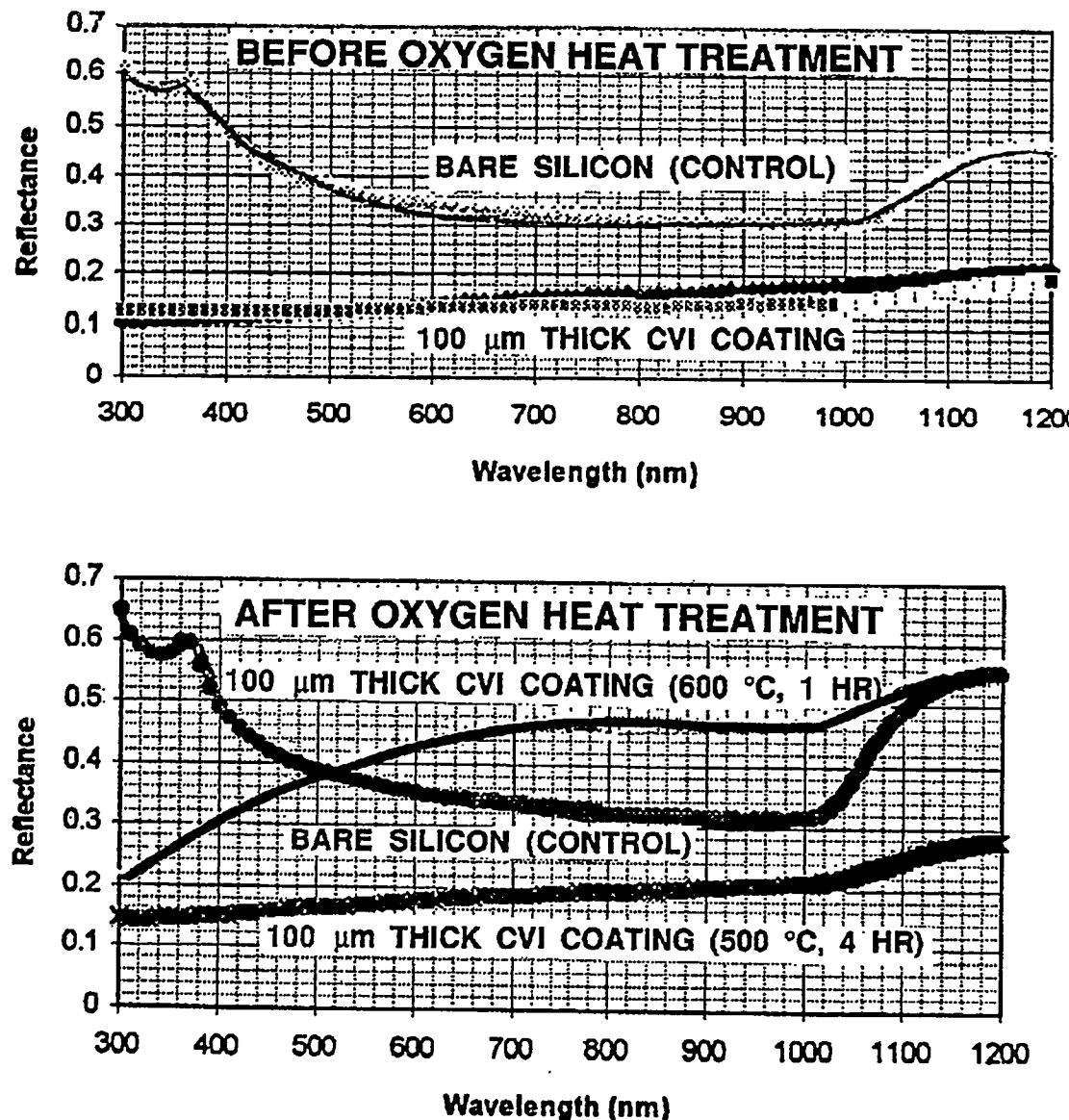


**Figure 19.** Reflectance from 100  $\mu\text{m}$  thick diamond composites on polished, mirror-like silicon substrates from the hot filament-assisted reactor. Transmittance in the visible range can be deduced from measured reflectance off the polished silicon substrate A. before and B. after treatment in an oxygen tube furnace for 1 hr. at 600  $^{\circ}\text{C}$  and 4 hr at 500  $^{\circ}\text{C}$ .

# **INFRARED ABSORPTANCE**

## **THROUGH HOT FILAMENT CVI DIAMOND COATINGS**

### **ON SILICON SUBSTRATES**

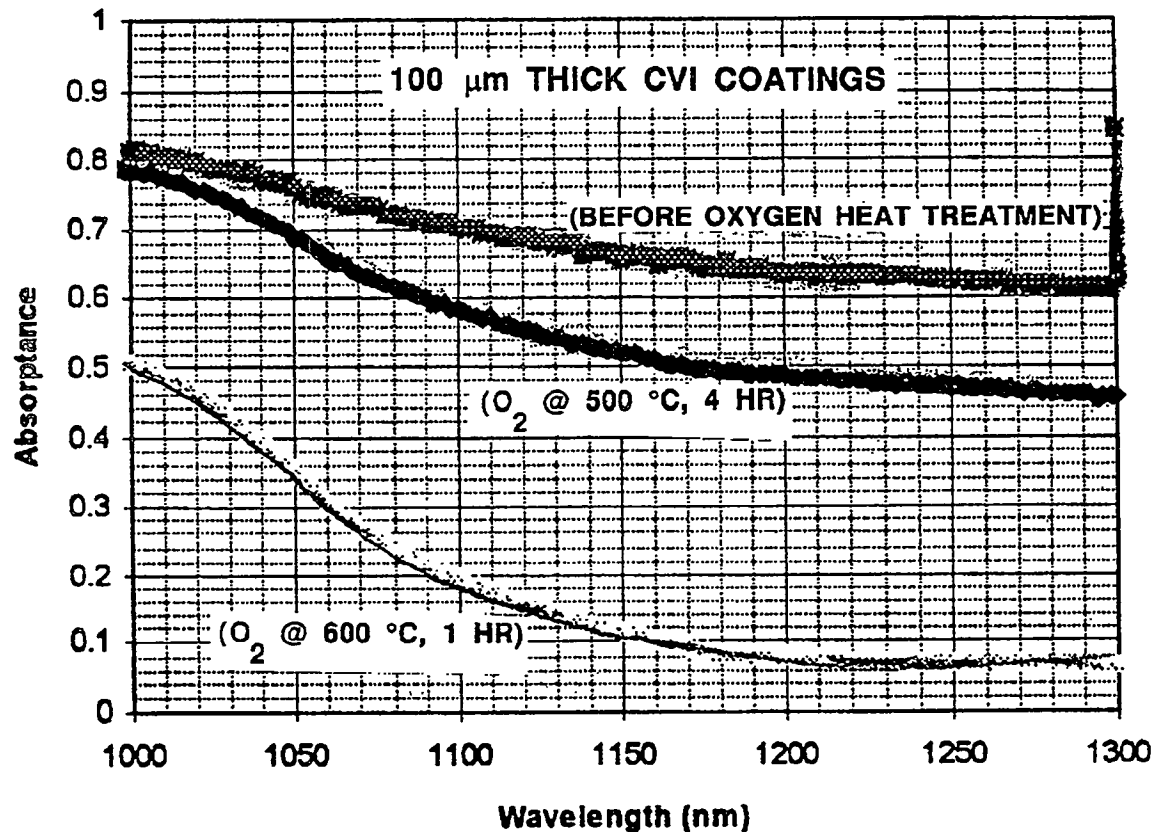
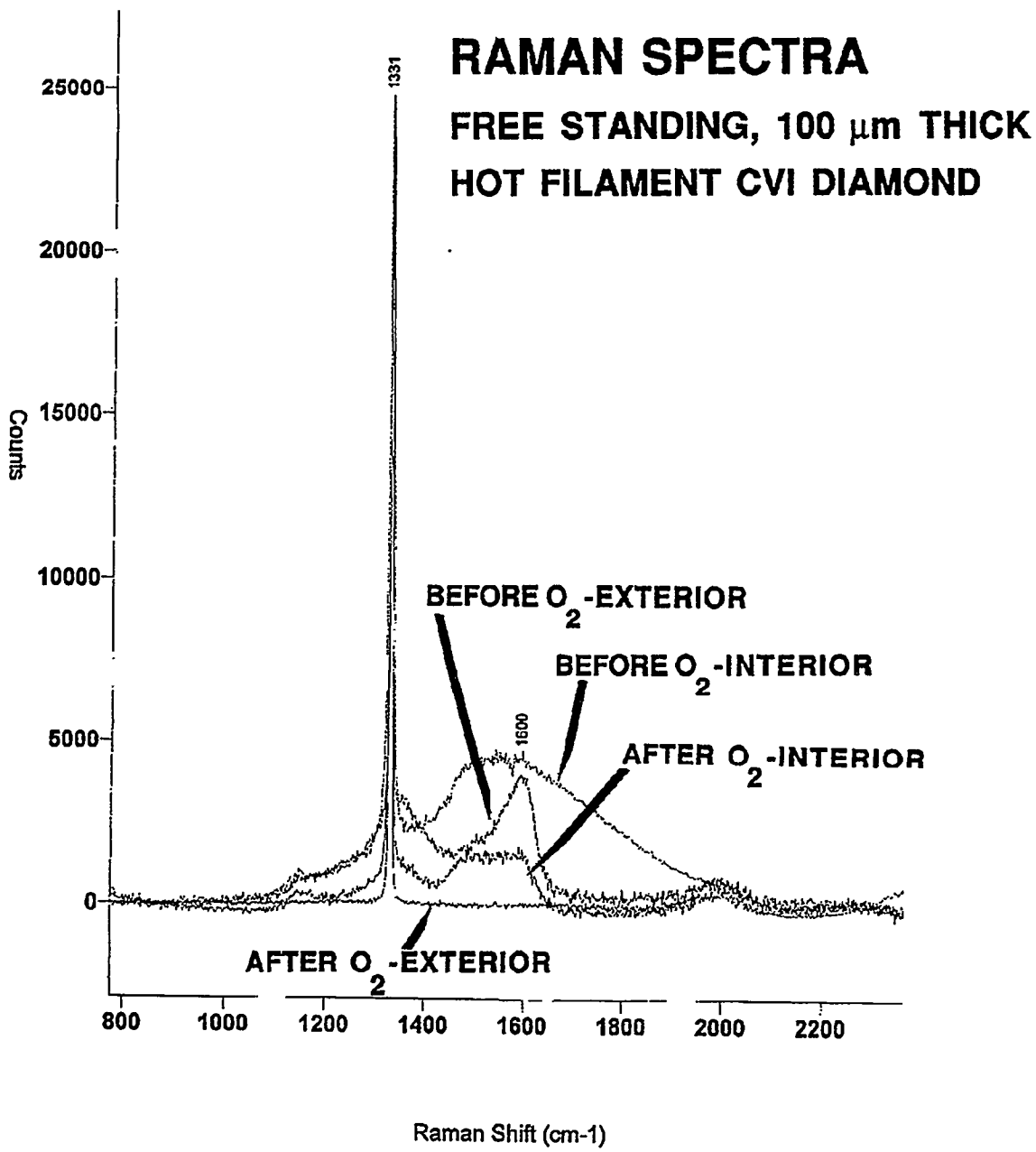


**Figure 20.** Infrared absorptance of diamond composite coating/substrate substrate “windows.” The 600  $^{\circ}\text{C}$  oxygen treatment increased transmittance substantially.



File # 3 BDLCP5X

**Figure 21.** Raman spectra from the exterior surface (reactor working gas side/oxygen flow side) and the interior surface (substrate side-tube furnace quartz pallet side) of freestanding diamond composites produced by the hot filament-assisted reactor. Substantial amounts of non-diamond carbon are selectively removed from both sides of the hot filament-assisted reactor sample that was exposed to oxygen at 600 °C for one hour.

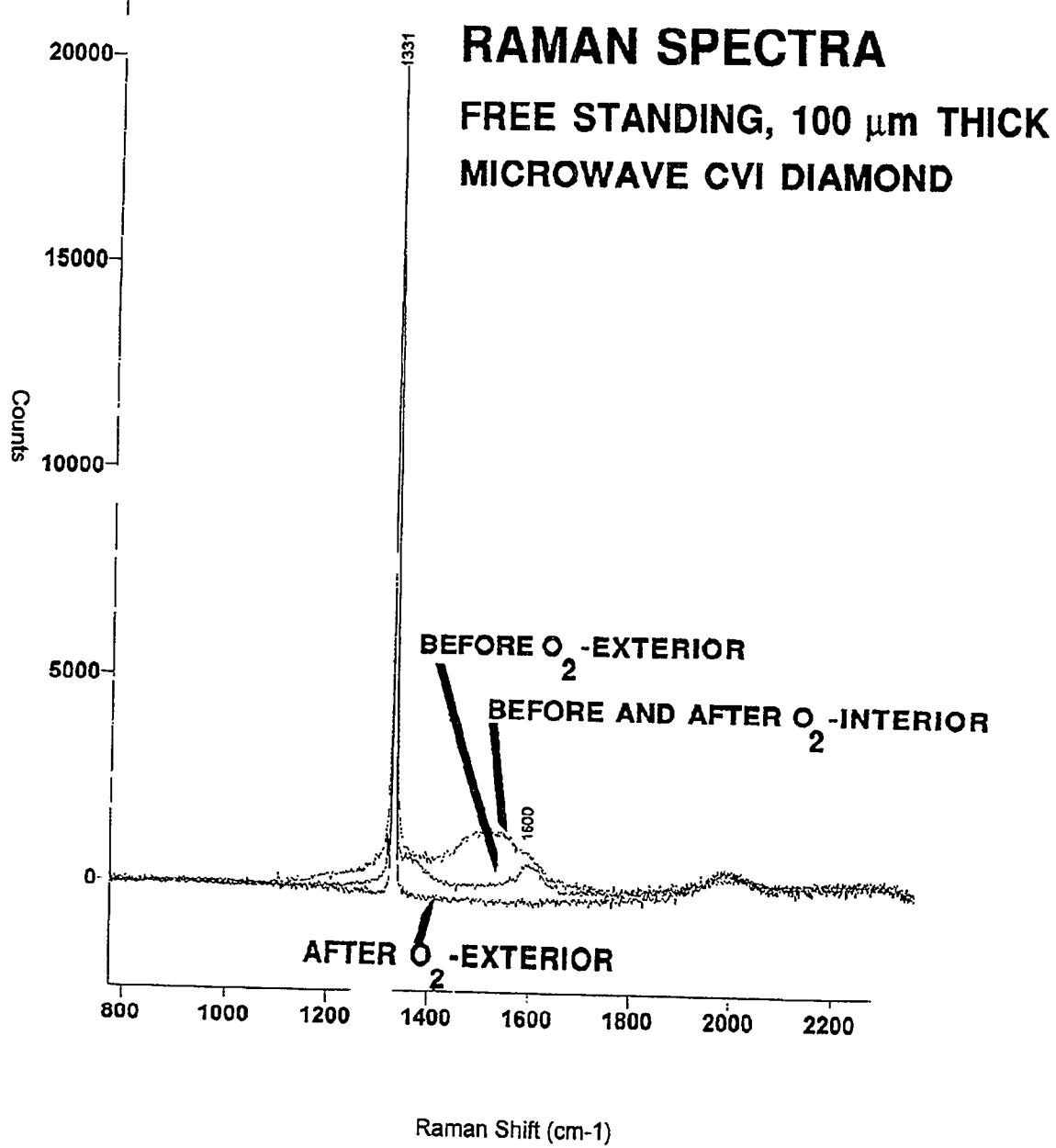
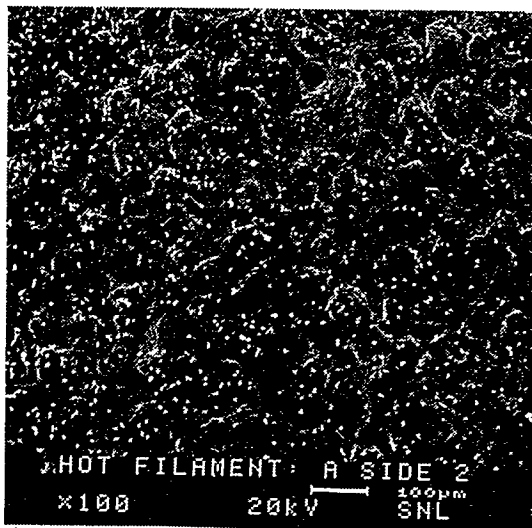
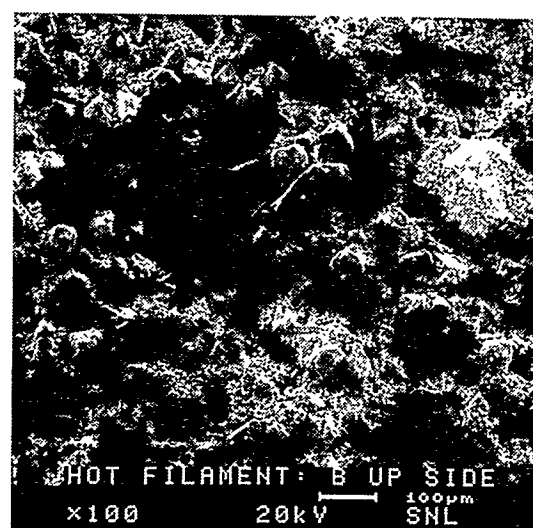


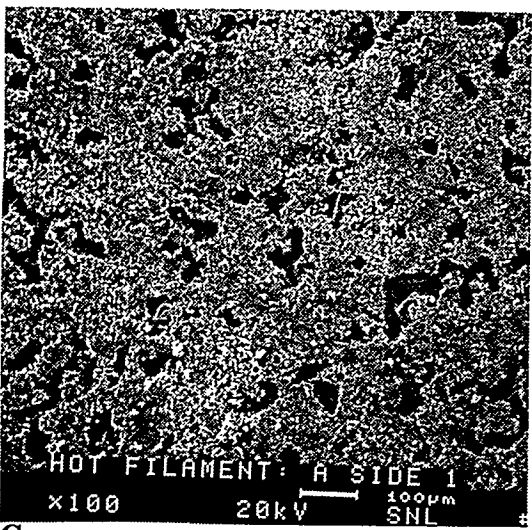
**Figure 22.** Raman spectra from the exterior surface (reactor working gas side/oxygen flow side) and the interior surface (substrate side-tube furnace quartz pallet side) of freestanding diamond composites produced by the microwave plasma-assisted reactor. Substantial amounts of non-diamond carbon are selectively removed from the exterior surface of the microwave plasma-assisted reactor sample that was exposed to oxygen flow at 600 °C for one hour.



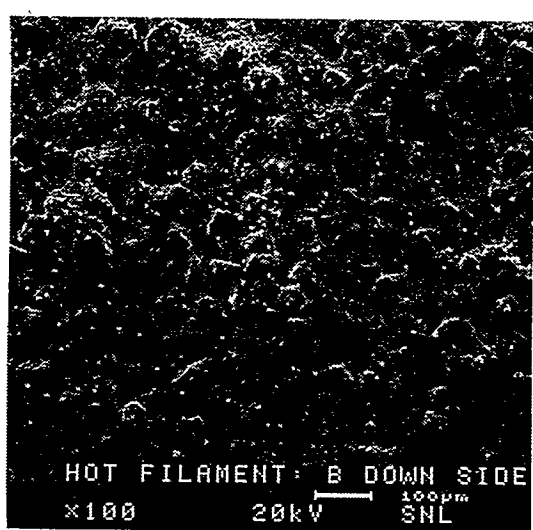
A



B



C



D

**Figure 23.** SEM micrographs showing a free-standing composite from the hot filament-assisted reactor before and after a 600 °C 1 hr oxygen tube furnace treatment. As a result of this treatment, the color of this sample changed from grey to white. **A.** Exterior surface, before; **B.** Exterior surface, after; **C.** Interior surface, before; **D.** Interior surface, after.

We searched for evidence that the diamond we were producing could produce sizable field emission currents at low fields. If we could observe this, then we would know that our samples had a low work function and we would be inclined to suspect that our samples might also exhibit negative electron affinity. We observed no discernible electron current from approximately one square centimeter sized samples biased up to -2 KV relative to a grounded aperture plate placed a millimeter parallel to the sample. The test system was capable of detecting currents in the nanoamp range.

### 3. Electron beam excited fluorescence

Natural, non-mined and CVD diamond may contain characteristic impurities or defects that give rise to fluorescence. Many of the samples we produced, especially those coming from the microwave plasma assisted reactor, fluoresced when evaluated with Raman spectroscopy. In view of the current strong interest in developing materials for flat screen displays, we mounted a few representative samples in an electron microprobe, and progressively increased the beam energy with the hope of discovering a novel, useful phosphor. Some small spots of electron-beam activated fluorescence lit up at beam energy from 2000 to 5000 eV. Unfortunately, no samples displayed fluorescent activity competitive with the low (< 10 eV) threshold energies sufficient to excite zinc oxide.

### 4. Density

Representative samples were taken to the Center for Microengineered Ceramics at the University of New Mexico where there are a variety of open-celled and close-celled porosimeters. After some amount of time, the samples were returned to us with the verbal report that judging from SEM micrographs, the samples were too dense to evaluate using the university's porosimeters.

Gravometric measurements indicated the best quality 100 mm thick composites from the hot filament-assisted reactor were approximately 85% the density of diamond.

## SUMMARY AND CONCLUSIONS

We have demonstrated that it is possible to form good quality, thick, relatively stress free, diamond coatings in relatively short amounts of time by first electrophoretically depositing or screen printing a porous diamond powder coating, then filling in the pores with CVI diamond. A hot filament-assisted reactor and a microwave plasma-assisted reactor were used to densify the composites.

Composites densified in each reactor exhibited several similar characteristics. Stronger composites formed from denser green ceramic diamond powder precursors. When silicon was used as a substrate material, extensively densified composites adhered strongly to the substrate. When nickel or molybdenum were used as substrates, strong freestanding pieces of diamond could be removed from the substrates after densification. The composite exteriors characteristically contained large amounts of diamond and some glassy carbon. The composite interiors and predominantly CVD diamond formed adjacent to the composites contained large amounts of diamond combined with diamond-like carbon.

Certain material properties depended on reactor conditions. Composites processed in the hot filament-assisted reactor densified more readily than those processed in the microwave plasma-assisted reactor. Composites formed in the microwave-assisted reactor were sealed over by a tight surface skin before densification was complete. The process window yielding deposits with high concentrations of diamond was larger when methyl fluoride plus hydrogen was used; lower concentrations were obtained when methane plus hydrogen was used as a working gas in the microwave plasma-assisted reactor.

The optical transmittance of diamond composites deposited in the hot filament-assisted reactor could be substantially improved by heat treating the samples in an oxygen tube furnace for one hour at 600 °C. The color of the treated samples changed substantially from grey to white. Forming CVI diamond composites, then burning off poor quality diamond and non-diamond carbon in oxygen and repeating these two steps may represent a commercially viable process for forming thick diamond windows and free-standing pieces of high quality diamond for other applications.

## REFERENCES

1. R. M. Chrenko and H. M. Strong, Physical Properties of Diamond, Technical Report No. 75CRD089, Oct. 1975, General Electric Company, Corporate Research and Development, Schenectady, N. Y.
2. K. E. Spear, J. Am. Ceram. Soc. 72, 171 (1989).
3. C. V. Cooper and C. Beetz, Jr., Surface and Coatings Technology, 47, 375 (1991).
4. S. Jin, J. E. Graebner, M. McCormack, T. H. Tiefel, A. Katz and W. C. Dautremont-Smith, Nature, 362, 822 (1993).
5. K. Higuchi and S. Noda, Diamond and Rel. Mat., 4, 220 (1992).
6. P. R. Chalker, A. M. Jones, C. Johnson and I. M. Buckley-Golder, Surface and Coatings Technology, 47, 365 (1991).
7. Stephen J. Harris and Anita M. Weiner, J. Appl. Phys. 70, 1385 (1991).
8. W. D. Kingery, Introduction to Ceramics, John Wiley and Sons, Inc. New York, (1967) p 34.
9. D. M. Tung, W. L. Hsu and K. F. McCarty, "Characteristics of Diamond Films Deposited in a Microwave Plasma", Proceedings of the First International Symposium on Diamond and Diamond-Like Films at the 175th Meeting of the Electrochemical Society, Los Angeles CA, May 7 - 12. 1989, ed. J. P. Dismukes et. al., Vol. 89-12, publ. Electrochemical Society, Inc., Pennington, NJ, p 500.
10. B. B. Pate, C. Bandis and D. Haggerty, J. Vac. Sci. and Technol., A, 12, 4, Pt 1, (Jul./Aug. 1994) 1607.

DISTRIBUTION:

1	MS 1082	David W. Palmer, 1333
1	MS 1409	A. D. Romig, Jr., 1800
1	MS 0343	Jim Borders, 1823
4	MS 0343	David R. Tallant, 1823
1	MS 0340	Michael Dugger, 1832
1	MS 0333	Alan J. Hurd, 1841
10	MS 0333	Janda K. Panitz, 1841
1	MS 0960	Jimmie Search, 2400
1	MS 0958	John Ledman, 2471
4	MS 0958	David Staley, 2471-2
1	MS 0959	Frank P. Gerstle, Jr., 2476
1	MS 9054	William McLean, 8300
4	MS 9162	Wen L. Hsu, 8431
4	MS 9162	Ciaran Fox, 8341
4	MS 9162	Mark McMaster, 8347
1	MS 9162	Arthur Pontau, 8347
1	MS 0894	Robert Williams, 9136
1	MS 0957	Gerald Cessac, 9199
1	MS 0357	Robert B. Asher, 9835
1	MS 9087	Central Tech Files, 8523-2
5	MS 0899	Technical Library, 13414
1	MS 0619	Print Media, 12615
2	MS 0100	Document Processing, 7613-2 For DOE/OSTI

